NASA Contractor Report 177551

USAAVSCOM Technical Memorandum 90-A-005

Airloads, Wakes, and Aeroelasticity

Wayne Johnson
Johnson Aeronautics
P.O. Box 1253
Palo Alto, California

NASA

National Aeronautics and
Space Administration

Ames Research Center
Moffett Field, California 94035-1000

US ARMY
AVIATION
SYSTEMS COMMAND

AVIATION RESEARCH AND
TECHNOLOGY ACTIVITY
MOFFETT FIELD, CA 94035-1099

AIRLOADS, WAKES, AND AEROELASTICITY

by
Wayne Johnson
Johnson Aeronautics
Palo Alto, California USA

SUMMARY

Fundamental considerations regarding the theory and modeling of rotary wing airloads, wakes, and aeroelasticity are presented. The topics covered are: (a) airloads and wakes, including lifting-line theory, wake models and nonuniform inflow, free wake geometry, and blade-vortex interaction; (b) aerodynamic and wake models for aeroelasticity, including two-dimensional unsteady aerodynamics and dynamic inflow; and (c) airloads and structural dynamics, including comprehensive airload prediction programs. Results of calculations and correlations are presented.

LIST OF SYMBOLS

c_l	section lift coefficient
C_T	rotor thrust coefficient, $T/\rho(\Omega R)^2(\pi R^2)$
M	Mach number
R	blade radius
r	blade spanwise coordinate
r_c	tip vortex core radius
T	rotor thrust
V	flight speed
Γ	bound circulation, vortex strength
μ	advance ratio, $V/\Omega R$
ρ	air density
σ	rotor solidity (ratio of blade area to disk area)
ψ	rotor blade azimuth angle
Ω	rotor rotational speed

1. INTRODUCTION

The objective of this lecture is to present the fundamentals of rotary wing airloads, wakes, and aeroelasticity. It is an exposition rather than a survey, focussing on concepts and results, for it is the implementation of these models that is complex, not their mathematics. The results presented are from the author's experience. The identification of the principal factors involved is general, but it is not meant to imply that this is the only way to develop the models. The topics covered are airloads and wakes, aerodynamic and wake models for aeroelasticity, and airloads and structural dynamics. Airloads and wakes are the principal subject. Background information and additional details can be found in references 1-9.

A helicopter rotor has low disk loading and low solidity (ratio of blade area to disk area) in order to achieve high hover efficiency. Hence the rotary wing is characterized by high aspect-ratio rotor blades, for both aerodynamic and structural behavior. A three-dimensional wing trails vorticity into the wake. For a helicopter, this vorticity is mainly in the tip vortices, trailed in helices below the disk for hover. In hover the axial convection is produced by the self-induced velocities of the wake. In forward flight, the helical tip vortices are convected rearward as well as downward, so the wake consists of concentrated tip vortices trailed in skewed interlocking helices (figure 1). The vortex wake of the rotor is a factor in most problems of helicopters, including performance, blade loads, vibration, and noise. An accurate calculation of the wake-induced nonuniform inflow and the resulting loading is needed in order to predict these aspects of the rotor behavior.

The strong, concentrated tip vortices dominate the rotor wake. They produce highly nonuniform induced velocity at the rotor disk, as the blades encounter vortices from preceding blades. The vortex-induced loading is a principal source of higher harmonic airloads on the blades. Figure 2 (from ref. 10) illustrates the behavior of the airloading, which is relatively consistent for all rotors. At low speed, there are loading changes on the advancing and retreating sides of the disk, caused by tip vortex encounters. Correlation with the locus of the tip vortex from the preceding blades shows that this impulsive loading at the tip is blade-vortex interaction (bvi). At high speed, negative loading on the advancing tip is common, as a consequence of flap moment balance with stall-limited loads on the retreating side. Bvi is still evident on the advancing and retreating sides. The locus of the tip vortex indicates again that the impulsive load on the advancing tip is bvi, but the impulse

has the opposite sign as at low speed. Hence the negative lift region on the advancing side must be producing substantial negative vorticity in the wake.

The aerodynamic and wake models used to calculate forward flight airloads in a modern comprehensive analysis typically have the following features. The rotor aerodynamic model is based on lifting-line theory, using steady two-dimensional airfoil characteristics and a vortex wake. Each blade section acts as a two-dimensional airfoil, with the wake influence contained in the wake-induced velocity. The section aerodynamics include empirical dynamic stall models, corrections for yawed or swept flow, and unsteady aerodynamic forces from thin-airfoil theory. The induced velocity can be obtained from momentum or vortex theory, resulting in blade-element theory for rotors. This model will be labeled "uniform inflow" here, although it likely includes a linear gradient of the velocity over the disk as well. For accurate forward flight airloads, the induced velocity should be obtained from a nonuniform inflow calculation, which is a numerical problem for rotors because of the complex wake geometry. The wake model for nonuniform inflow is based on a vortex lattice (straight-line segment) approximation, with a small viscous core radius used for the tip vortices, and some model of the wake rollup process. The wake geometry models include simple undistorted geometry ("rigid") and calculated free wake geometry.

2. AIRLOADS AND WAKES

This section describes lifting-line theory for rotary wings, including a practical implementation and a consideration of the blade section aerodynamic model. The rotor wake model is described, including the free wake geometry and a discussion of blade-vortex interaction.

2.1. Lifting-Line Theory for Rotary Wings

2.1.1. Forward flight airloads calculations. Forward flight airloads calculations are generally based on lifting-line theory. It is essential to have the capability to treat viscous and compressible flow effects, which are present to some degree in almost all helicopter operating conditions. This is accomplished in lifting-line theory by using experimental data for the two-dimensional airfoil characteristics, hence the continuing utility of lifting-line theory for rotor aerodynamics. The assumptions of lifting-line theory are generally well satisfied for rotor blades: that the wing has a high aspect-ratio, or more generally that the spanwise variation of the aerodynamic environment is slow. Lifting-surface theory is more accurate in the treatment of three-dimensional and perhaps compressible flow effects at low angle-of-attack, but inviscid lifting-surface theory is no more accurate than lifting-line theory at high angle-of-attack. Computational fluid dynamics methods are beginning to be applied to helicopter rotor flows in the depth needed for airloads calculations, i.e. encompassing wake formation and interaction, blade moment and drag, and coupling with the dynamics. Lifting-line theory contains so many approximations and assumptions that ultimately it must be replaced by a more accurate method. Presently however, lifting-line theory remains the most practical (efficient and reasonably accurate) method for including viscous effects in the rotor analysis.

2.1.2. Basics of lifting-line theory. The assumption of high aspect-ratio splits the three-dimensional wing aerodynamic problem (unsteady, compressible, and viscous) into inner and outer problems, i.e. wing and wake models (figure 3). The outer problem is the wake: trailed and shed vorticity behind the lifting-line (bound vortex). The inner problem is a two-dimensional airfoil, or more correctly an infinite wing in a uniform, yawed free stream. These problems are connected through the wake-induced velocity and the bound circulation. The outer problem calculates the induced velocity components at the wing, from a wake with strength determined by the bound circulation. Note that the induced velocity is not needed at an arbitrary point, just at the lifting-line. The inner problem calculates the bound circulation from the aerodynamic environment, with the wake-induced velocity included in the free stream. Note that the pressure on the wing is not needed, just the bound circulation (and the section lift, drag, and moment in order to calculate performance and couple with the structural dynamics).

The assumption of high aspect-ratio has the following consequences, comparing the lifting-line problems to the full solution. The inner problem has simpler geometry (two-dimensional) but complex flow (Navier-Stokes equations). In the outer limit the inner solution can be considered irrotational. The outer problem has complex geometry (the vortex wake) but irrotational flow. In the inner limit the outer solution has simple geometry. In the matching domain there is both simple geometry and irrotational flow.

Uniform inflow from momentum or vortex theory is an approximation for the solution of the outer problem (the wake). This approximation introduces effects requiring additional treatment, particularly the tip loss factor.

2.1.3. Perturbation theory. Formal lifting-line theory is the solution of the three-dimensional wing loading problem using the method of matched asymptotic expansions. Based on the assumption of large wing aspect-ratio, the problem is split into separate outer (wake) and inner (wing) problems, which are solved individually and then combined through a matching procedure. For the rotor in forward flight, it is necessary to consider wings with swept and yawed planform, in unsteady, compressible, and viscous flow.

2

The lowest-order fixed wing solution is Prandtl's theory (steady and no sweep). Development of higher-order lifting-line theory originated with Weissinger for intuitive methods, and with van Dyke for singular perturbation methods. The lifting-line theory developments found in the literature, although including higher orders, unsteady, transonic, and swept flow, are generally analytical methods. They obtain analytical solutions for both the inner and outer problems, and are in quadrature rather than integral form. Often the inner solution is inviscid, or even a thin airfoil. These theories are not therefore directly applicable to rotors, but do provide a guide and sound mathematical foundation for the rotary wing development.

For the rotary wing, it is necessary to include stall (high angle-of-attack) in the inner solution, and the helical, distorted, rolled-up wake geometry in the outer solution. Hence for rotors the objective is to obtain from lifting-line theory a separate formulation of the inner and outer problems, with numerical not analytical solutions, and a matching procedure that will be the basis for an iterative solution. A key consideration is the need to retain the two-dimensional airfoil tables in the inner solution, for the viscous effects. Hence whatever approximations that are required to retain the tables will be accepted. Furthermore, a practical method is needed, one that gives good accuracy without convergence problems or singularities.

2.1.4. Second-order lifting-line theory. Higher order theory is considered in order to improve the calculation of the airloads without actually resorting to lifting-surface or CFD methods, which require more computation and still need some development for rotary wing applications. Several investigations have shown that second-order lifting-line theory gives nearly the same results as lifting-surface theory, including the lift produced in close blade-vortex interactions. In addition, second-order theory should also improve the loads calculations for swept tips, yawed flow, and low aspect-ratio blades.

In the second-order outer problem (the wake), the wing is a dipole plus a quadrupole, which for a thin airfoil (with no thickness or camber) is equivalent to a dipole at the quarter-chord. The dipole solution is a wake of vortex sheets.

In the second-order inner problem (the wing), the boundary condition at infinity includes a wake-induced velocity that varies linearly in space. For a thin airfoil, the same lift is obtained with a uniform induced velocity, by using the value at the three-quarter-chord. The correct moment is not obtained however, since a linear induced-velocity variation over the chord produces a moment about the quarter-chord, but a uniform induced-velocity does not. In general, it is necessary to define a remainder solution that is the second-order solution after accounting for the induced-velocity at the three-quarter-chord. This remainder solution will be ignored in practice, so it becomes an error estimate. The lift error is found to be small, and the moment error also except for the moment about the quarter-chord produced by a linearly-varying induced-velocity.

In order to retain use of the airfoil tables, the only parts of the second-order theory that can be used are placing the lifting-line at the quarter-chord and the collocation point at the three-quarter-chord.

2.1.5. Integral equation formulation. The perturbation solution procedure alternates between the inner and outer problems, using only the solution up to the previous order. Combining and solving all orders simultaneously is equivalent in terms of the perturbation expansions. It is natural to combine the inner problems. The lowest order inner problem is the airfoil with just geometry boundary conditions, and the first order inner problem has the wake-induced velocity boundary conditions. These are easily combined since the wake just gives an angle-of-attack change.

Combining the outer problems means evaluating the induced-velocity using the total bound circulation, from the combined inner problem rather than just from the lowest order inner problem. This changes the nature of the solution, from direct quadrature to an integral equation. It is necessary to invert the integral equation, but with airfoil tables an iterative solution is required anyway. Moreover, it is found that the solution of the integral equation is well behaved, while the direct solution is singular at the wing tips for normal wing planforms.

2.1.6. Comparison of formulations. A consideration of the simplified inner problem will show the differences between the common formulations of lifting-line theory. Let θ be the geometric angle-of-attack of the wing section. The inner problem solution (static, with no sweep) can be analytical or numerical:

$$\text{analytical, thin airfoil:} \qquad \frac{\Gamma}{\pi c} = U\theta - v$$

$$\text{numerical, airfoil tables:} \qquad \frac{\Gamma}{\pi c} = \frac{U}{2\pi} c_l(\theta - v/U)$$

where Γ is the bound circulation, c the chord, U the free stream velocity, $c_l(\alpha)$ the lift-coefficient as a function of angle-of-attack, and v the wake-induced velocity. The outer problem can obtain the induced velocity v at the quarter-chord or three-quarter-chord, by integrating the effects of all wake vorticity (excluding the bound vortex). For example, a thin planar wake gives:

$$v_{c/4} = \frac{1}{4\pi} \int \frac{d\Gamma/d\eta \; d\eta}{y - \eta}$$

The following implementations of lifting-line theory are of interest.

a) First-order perturbation theory obtains v from $\Gamma_0 = \pi c U \theta$:

$$\frac{\Gamma}{\pi c} = U\theta - v_{c/4}(\theta)$$

b) Prandtl's integral equation is first-order, but obtains v from Γ:

$$\frac{\Gamma}{\pi c} = U\theta - v_{c/4}(\Gamma)$$

c) A common implementation for rotors is the first-order theory, but using airfoil tables:

$$\frac{\Gamma}{\pi c} = \frac{U}{2\pi} c_l(\theta - v_{c/4}(\Gamma)/U)$$

d) A second-order implementation uses v at the three-quarter-chord:

$$\frac{\Gamma}{\pi c} = \frac{U}{2\pi} c_l(\theta - v_{3c/4}(\Gamma)/U)$$

e) Weissinger's L-theory includes the contribution of the bound vortex in evaluating v at the three-quarter-chord, and equates the induced angle-of-attack to the geometric angle-of-attack. This is equivalent to using the thin-airfoil solution of the inner problem in second-order theory:

$$\left(\frac{\Gamma}{\pi c} + v_{3c/4}(\Gamma)\right) = U\theta$$

2.1.7. Sweep and yawed flow. Large sweep angles can be included in the second-order theory, but it is necessary to assume small curvature so the wake-induced velocity effects in the inner problem remain two-dimensional. For most rotor blades the curvature is small, except a kinks in the quarter-chord line. The analysis relies on the integral form and spanwise discretization to keep the loading well behaved at such kinks.

2.1.8. Unsteady loading. With unsteady motion and loading, the inner problem is an unsteady, two-dimensional airfoil with a shed wake, and the outer problem excludes both the bound vortex and the inner shed wake when calculating the induced velocity. It is natural to retain the shed wake in the outer rather than the inner problem, so that the shed wake and trailed wake can be treated identically, especially since subtracting the inner shed wake from the outer problem is difficult with the complex wake geometry of a rotor. Then the induced velocity from all vorticity (except the bound vortex still) is evaluated at the three-quarter-chord, and treated as a uniform flow for the inner problem. The shed wake is thus a boundary condition of the inner solution, not a part of the inner model.

The assumption that the shed wake-induced velocity is constant over the chord is a major approximation. With the induced velocity evaluated at a single point, the shed wake model must be modified to obtain the unsteady loads correctly. It is found that the Theodorsen and Sears functions (the shed wake effects in two-dimensional airfoil theory) are well approximated for low frequency (and reasonably well up to reduced frequencies of about 1.0) if the shed wake in the outer problem is created a quarter-chord aft of the collocation point, not at the bound vortex as for the trailed wake.

2.2. Practical Implementation of Lifting-line Theory for Rotors

Guided by the results of perturbation theory, the following is a practical implementation of lifting-line theory for rotors. The outer problem is an incompressible vortex wake behind a lifting-line, with distorted geometry and rollup. The lifting-line (bound vortex) is at the quarter-chord, as an approximation for the quadrupole line introduced by second-order loading. The trailed wake begins at the bound vortex. The shed wake is created a quarter-chord aft of the collocation point on the wing (the lifting-line approximation for unsteady loading). The three components of wake-induced velocity are evaluated at the collocation points, excluding the contributions of the bound vortex. The collocation points are at the three-quarter-

chord (in the direction of the local flow), as an approximation for a linearly-varying induced velocity introduced by the second-order wake.

The inner problem consists of unsteady, compressible, viscous flow about an infinite aspect-ratio wing, in a uniform flow consisting of the yawed free stream and three components of wake-induced velocity. This problem is split into parts: two-dimensional, steady, compressible, viscous flow (airfoil tables), plus corrections. The corrections account for unsteady flow (small angle-of-attack noncirculatory loads from thin airfoil theory, but without any shed wake); dynamic stall (some empirical model); swept and yawed flow (the equivalence assumption for a swept wing); tip flow; and perhaps blade-vortex interaction and Reynolds number.

This formulation is generally second-order (in the inverse of the aspect-ratio) accurate for lift, including the effects of sweep and yaw, but less accurate for section moments (which are basically still first-order). In particular, with typical blade-vortex separations, second-order lifting-line theory is as accurate as lifting-surface theory for lift calculations.

2.3. Rotor Blade Section Aerodynamic Model.

For the blade section aerodynamic model (the inner problem) it is important to account for large angles and reverse flow; transformation of the loads in bent-blade/wind axes (the section lift and drag) to hub axes; and radial drag. Radial drag is typically obtained by assuming that the total viscous drag force on the section (vector addition of the radial and chordwise components) has the same direction as the local yawed flow.

Tip flow corrections include a tip loss factor, compressible tip relief (a small reduction in effective Mach number), and the effects of a swept tip (discussed below). The tip loss factor is needed for blade-element theory, when the induced velocity is obtained from momentum theory. For nonuniform inflow a tip loss factor is not appropriate, but it is necessary to consider the radial station of the rolled-up tip vortex when it reaches the trailing edge of the blade.

Yawed and swept flow require significant aerodynamic corrections. The inner problem is an infinite wing with yaw and sweep (the planform is defined relative to a straight span-line, so radial velocity in forward flight produces yawed flow, while sweep is obtained from the locus of the quarter-chord relative to the span-line). The section loads are obtained from airfoil tables that give the solution for a wing no yaw or sweep, using the equivalence assumption for swept wings. The objective is to derive equivalent angle-of-attack and Mach number for evaluating the coefficients, and corrections for the coefficients from the tables (and properly account for the chord and blade area when multiplying the coefficients by chord, dynamic pressure, and panel width in order to obtain the section loads). The principal assumptions are:

a) The lift-curve-slope is not affected by spanwise flow.
b) The Mach number normal to the (swept) quarter-chord defines compressibility effects.
c) The angle-of-attack and chord in the local flow direction define the drag and stall.
d) The net drag force is in the local flow direction, so the radial drag component can be obtained from the section drag coefficient.

Corrections for the effective shape and thickness of the airfoil in yawed flow are seldom used. Probably the airfoil tables should correspond to the shape of the cross-section in the local flow direction. Hence for hover, the shape perpendicular to a straight reference line is appropriate. In forward flight however, the yaw direction varies with azimuth. Fortunately, over most of the disk the yaw angle is not too large, so the absence of any correction for effective shape and thickness does not appear to produce any worse errors than the other approximations of the model. Note that if the yaw angles are large, then first-order lifting-line theory breaks down too.

Swept tips introduce other considerations as well. The inertial load acts at the blade section center-of-gravity, and the aerodynamic load acts at the quarter-chord (actually, the airfoil table reference). These loads produce bending and torsion of the blade relative to the swept elastic axis.

2.4. Wake Models

2.4.1. Rotor wake vorticity. A three-dimensional wing trails the bound circulation Γ into a wake. The radial variation of Γ produces trailed vorticity, parallel to the local free stream direction at the time it leaves the blade. Azimuthal variation of Γ produces shed vorticity, oriented radially. The strength of the trailed and shed vorticity is determined by the radial and azimuthal derivatives of Γ at the time the wake element left the blade. The bound circulation has a peak near the tip, and quickly drops to zero. The trailed sheet therefore has a high strength (proportional to the radial derivative of Γ) at the wake outer edge, and quickly rolls up to form a concentrated tip vortex. This rollup process, which is also influenced by the tip geometry, produces a line vortex with a small core radius, hence large velocities.

The vorticity in the tip vortex is distributed over a small but finite region, called the vortex core, because of viscosity of the fluid. The core radius is defined at the point of maximum tangential or circumferential velocity. The vortex core is an important factor in the induced velocity character since it limits the maximum velocities near the tip vortices. There is only limited experimental data on the core size, especially for rotors.

The gradient of bound circulation is low at the root of a rotor blade, so the root vortex is weaker and more diffuse. Between the tip and root vortices there is an inboard sheet of trailed vorticity, the outboard portion of which may roll up into a weak vortex as well. In forward flight this inboard sheet has shed vorticity, from the azimuthal derivative of Γ.

2.4.2. Rotor wake geometry. The trailed and shed vorticity is left in the fluid as the blade rotates, and then is convected with the local fluid velocity, consisting of the free stream (i.e. the helicopter translation in forward flight) and the wake self-induced velocity. The wake is convected downward (normal to the disk plane) by the mean induced velocity and free stream, and aft in forward flight by the inplane component of the free stream. The self-induced velocity produces substantial distortion of the vortex filaments as they are convected. The wake geometry thus consists of distorted, interlocking helices, one behind each blade, skewed aft in forward flight.

2.4.3. Nonuniform inflow. The strong, concentrated tip vortices trailed in helices from each blade are the dominant feature of the rotor wake. Because of the rotation, the blade encounters the vortex from the preceding blade, in both hover and forward flight. The tip vortices produce a highly nonuniform flow field through which the blades must pass. In forward flight, the wake is convected downstream, so tip vortices are swept past the entire rotor disk (rather than remaining in the tip region as in hover). Close vortex-blade encounters occur primarily on the sides of the disk, where the blade tip sweeps over the vortices. When there is a close passage, the vortex produces large velocities and hence large loads on the blade. This vortex-induced loading is a principal source of higher harmonic airloads. The nonuniform induced velocity has an overall variation over the disk, roughly linear in forward flight, plus large local variations produced by the blade passing close to tip vortices from preceding blades. The blade loads in forward flight show loading changes on the advancing and retreating sides (figure 4), caused by the tip vortex encounters, which depend highly on the flight condition.

2.4.4. Wake rollup process. Typically the wake rollup process is modeled not calculated, meaning that the structure and properties of the rolled-up wake are determined from assumptions and input parameters, and from the spanwise distribution of the bound circulation where the wake was created. It is important that the model account for the influence of (a) the strength of the tip vortex when it encounters the following blade; (b) the core radius when the vortex is fully rolled up; and (c) the effect of the vortex rollup on the tip load of the generating blades.

A calculation of the wake rollup from first principles is needed, but it is a difficult problem, beginning to be attacked using the methods of computational fluid dynamics (for example, ref. 11). The vortex core is largely formed at the blade trailing edge, so the problem is not the inviscid rollup of a vortex sheet. Moreover, discretization of the wake for a rollup calculation is not easy; indeed it may not be well posed even for an inviscid, two-dimensional problem. Hence the rollup problem involves three-dimensional, unsteady, viscous fluid dynamics. Currently airloads calculations must rely on models of the rollup process.

The wake model must encompass the rollup implied by typical circulation distributions on rotor blades. Generally it is assumed that the lift is concentrated at the tip of the rotating wing, because of the large dynamic pressure there produced by the rotation. So the trailed vorticity strength is high at the outer edge of the wake, and the vortex sheet quickly rolls up into a concentrated tip vortex. The formation of the vortex is influenced by the tip geometry, with the core largely formed by the time the vortex leaves the trailing edge. The rolled-up tip vortex quickly attains a strength nearly equal to the maximum bound circulation. The tip vortex has a small core radius, depending on the blade geometry and loading. There is an inboard vortex sheet of trailed vorticity, with opposite sign as the tip vortex. Since the gradient of bound circulation is low inboard, the root vortex is weaker and more diffuse. This is the assumed picture of the rollup process upon which the wake model is based.

In relating the rolled-up wake structure to the bound circulation distribution, it is necessary to consider single-peak and dual-peak cases. For the lifting rotor in hover and low speed forward flight, the bound circulation is positive along the entire span; this is the single-peak case. There will be local minima and maxima in Γ from bvi, but generally there is a monotonic increase and decrease in Γ, with a peak near the tip.

It is common for a helicopter rotor in high speed forward flight to encounter negative lift on the advancing tip, particularly in the second quadrant (see figure 2). With a flapping rotor, the net pitch and roll moment on the hub must be small (zero if there is no flap hinge offset). In forward flight, the lift capability on the retreating side is limited by the combination of low dynamic pressure and stall of the airfoil. Consequently the lift on the advancing side must also be small, in order to maintain roll balance. At sufficiently high speed, the lift on the advancing tip can become negative. Large twist of the blade (built-in or elastic) will increase the negative loading.

Over much of the disk Γ is still positive all along the span. However, there is a range of azimuth on the advancing side with a negative peak near the tip and a positive peak inboard; this is the dual-peak case. Here the tip vortex will form with negative strength (opposite sign as normal rollup), with a sheet of positive trailed vorticity created between the two peaks,

6

which perhaps rolls up to some extent also. Thus the wake model also considers the wake created by dual-peak span loading, perhaps with multiple rollup of the trailed vorticity. Figure 5 illustrates the wake structure.

The wake structure is often more complicated than considered by the single-peak and dual-peak models. For example, there are local minima and maxima in the bound circulation from bvi and reverse flow, and at low speed bvi can produce negative loading over a small portion of the rotor disk. Such structure has too much detail to be accommodated by a modeling approach; a calculation of the rollup is certainly needed.

The effects of the vortex rollup process on the tip loading of the generating blade should be considered. Most such effects are beyond lifting-line theory, but at least the radial location of the rollup should be modeled. The core is largely formed by the time the tip vortex reaches the trailing edge, even for a tapered tip. The center of the core is found somewhat inboard of the physical tip, typically 1% R inboard for a rectangular planform and more for a highly tapered tip. In lifting-line theory, this implies that there is no bound circulation of the blade tip outboard of the rolled-up location, with a significant effect on the spanwise loading distribution if the tip vortex forms at least 3-5% R inboard. This effect can be modeled by forcing the bound circulation to be dumped into the tip vortex at the proper (prescribed) radial location.

2.5. Nonuniform Inflow Calculation.

2.5.1. Wake-induced velocity. The nonuniform inflow is calculated by integrating the Biot-Savart law over the wake. Hence the induced velocities depend on the strength and geometry of the wake vorticity. The strength is defined by the radial and azimuthal variation of the bound circulation. The geometry can be obtained from several sources: (a) a simple assumed model, normally in forward flight the rigid geometry, using just the vertical convection by the mean induced velocity; (b) a prescribed model, based on measurements (mainly used for hover); or (c) a calculated free wake geometry.

Because of the basic helical geometry, it is not possible to evaluate the integrals analytically, even with no distortion. A direct numerical integration is not satisfactory wither, because the large variations in the integrand (produced by bvi) require small step sizes for accuracy. Hence the wake is modeled by a set of discrete elements. The Biot-Savart law can be integrated analytically for each element, and the total velocity obtained by summing contributions from all elements. This approach is both accurate and efficient. The calculation of nonuniform inflow is still a tremendous numerical problem, which was an early application of digital computers to helicopters. With current machines, nonuniform inflow calculations are practical for routine use in helicopter analyses.

2.5.2. Discretized wake model for calculations. The tip vortices are modeled as a connected series of straight line segments, with some kind of core representation. This is a good model for the most important part of the wake. The inboard trailed and shed vorticity is typically modeled as a vortex mesh or lattice, or possibly vortex sheet panels (sometimes the inboard wake is neglected entirely). With a lattice (line segment) model of the inboard wake, a large core size is needed, not as a representation of a physical effect, but to produce an approximation for the sheet element, by eliminating any singularities in the velocity for close passage of following blades. Note that a large core line element might also represent partially rolled-up trailed vorticity inboard or at the root.

Options for modeling the inboard wake panels include vortex sheets, either nonplanar-quadrilateral or planar-rectangular; or line segments in the middle of the panels, with a large core to eliminate singularities. The nonplanar-quadrilateral element is very expensive, and planar-rectangular elements introduce problems with mismatched edges. Moreover it is found that line segments give about the same results as sheet elements. Hence for economy line segments are used, producing a vortex lattice model. Such a model for the inboard wake is not as good as the tip vortex representation, but the inboard wake is not as important either, so a more approximate model is acceptable. If the inboard wake model is important for a case, then a better model for the rollup process will be needed too.

Modeling the wake by a set of discrete vortex elements introduces the following approximations: replacing the curvilinear geometry by a series of straight line or planar elements; simplified distribution of strength over an individual element (constant or linear); and sheets replaced by lines, or a planar-rectangle approximation for a nonplanar-quadrilateral. A practical model must balance the accuracy and efficiency of such approximations.

2.5.3. Development of the discretized wake model. The bound circulation Γ is calculated at discrete points on the disk, both radially and azimuthally. A linear variation of Γ between these points means the blade generates a wake of sheet panels (figure 6). The strength of the trailed and shed vorticity in a panel can be obtained from Γ at the time it was created (i.e. the circulation corresponding to the four corners of the panel). A radial change in Γ produces trailed vorticity, with the strength in the panel constant radially and linear along its length. An azimuthal change in Γ produces shed vorticity, with the strength in the panel constant azimuthally and linear along its length.

An economical approximation for the sheet panel is line segments, with a large core to avoid velocity singularities near the line. Hence a vortex lattice model is obtained by collapsing all wake panels to finite strength line segments (figure 7). The line segments are in the center of the sheet panel, so the points at which the induced velocity are calculated

(collocation points) are at the midpoints of the vortex lattice grid, both radially and azimuthally. Locating the collocation points midway between the trailers is a standard practice, to avoid the singularities at the lines. Locating the collocation points midway azimuthally is required to correctly obtain the unsteady aerodynamic effects of the shed wake (ref. 1).

With the sheets collapsed to lines, the strength of the line segments vary linearly along their length. A further approximation is stepped (piecewise constant) variation in strength. Then instead of a linear variation along the line, there is a jump in the strength at the center of the panel, where the shed and trailed lines cross. This wake model corresponds to a stepped distribution of the bound circulation over the disk, both radially and azimuthally. There is little reason to use such a stepped variation in strength, since the linear variation is as easy to implement. It is important to note that for a helicopter wake the principal issue is the approximation of sheet panels by lines, not the difference between stepped and linear variation of the bound circulation.

Consider the wake model behind the reference blade, where the induced velocity is being calculated, which will be called the near wake in this discussion (the terms "near wake" and "far wake" are used in many ways in the literature). The implementation of lifting-line theory involves primarily this portion of the wake. The most important requirement is to model the detailed variation of the wake strength, both radially and azimuthally, in order to accurately get the classical three-dimensional (Prandtl) and unsteady (Theodorsen) effects of the wake on the wing loading. The rollup process is less important for the near wake.

A vortex lattice is used for the near wake, rather than sheet elements. Discretization of the wake is better behaved using line segments than sheet elements. With sheet elements, numerical difficulties arise from the edge and corner singularities (particularly when planar-rectangular elements are used) and the fact that nonplanar-quadrilateral elements can not be integrated analytically. Also, the most important case of the downwash from the two sheet panels adjoining the collocation point would require a higher order element or some other special treatment.

The rollup process is not considered in modeling the near wake, except that the effect of the rollup on the tip load of the generating blade should be modeled. The radial location of the tip vortex formation can be prescribed, so the last trailed wake segment is placed at a spanwise station inboard of the tip (typically 1% R inboard for a rectangular tip). This forces the blade to dump the remaining bound circulation into the wake at that span station. The effect on the blade loading will be significant for a highly tapered tip, such as the ogee tip where the rollup occurs about 6% R inboard of the tip.

The geometry of the collocation points involves placing them at the three-quarter-chord in the local flow direction, in order to implement second-order lifting-line theory. Note that this geometry is part of the outer problem not the inner problem, i.e. the geometry of the wake rather than the blade. The wake geometry is obtained from the position of the lifting-line at the current and past time steps. Thus the wake geometry can be used to get the local flow direction for the collocation points. A consequence of this approach is that the collocation points are automatically kept away from trailed line segments of the near wake. With the highly distorted geometry of the rotor wake, especially near the reverse flow boundary, some close encounters between the collocation points and wake vortex lines can still occur. The calculation can use a core size for the near wake line segments in order to avoid singularities, but this core size has no physical significance, and indeed its value must not influence the solution for the loading.

Consider the wake when it reaches a following blade (where the induced velocity is being calculated), which will be called the far wake in this discussion. For the far wake, it is most important to model the rollup process. Since the wake quickly rolls up at the outer edge to form a concentrated tip vortex, the tip vortices play a dominant role in the aerodynamics, and must be modelled well. The inboard vorticity plays a lessor role, so more approximations are acceptable. The wake rollup process is modeled rather than calculated, which means that the structure and strength of the far wake are obtained from assumptions, applied to the form of the radial distribution of the bound circulation.

Consider the single-peak case, when the bound circulation has the same sign (positive or negative) radially for a given azimuth. The radial maximum of the bound circulation is Γ_{max}. It is assumed that in the far wake (i.e. where the rollup process is complete) there is a rolled-up tip vortex with strength equal to Γ_{max} of the azimuth where the wake was created. There is corresponding negative trailed vorticity with total strength $-\Gamma_{max}$ in the inboard sheet. The tip vortex model then is a line segment with this strength and a small core radius (which is an input parameter). Any error in the assumed strength, because the vortex is partially- or over-rolled up, will be compensated for by the value of the core radius. In the absence of a calculation of the strength and rolling up of the vorticity, the detailed structure of the inboard vortex sheet is unknown. Therefore the inboard portion of the wake is modeled as a single sheet panel with trailed and shed vorticity. It is assumed that the strength of the inboard trailed vorticity is constant radially, with a total value of $-\Gamma_{max}$. This is an efficient model, consisting of only two elements with three line segments at each azimuth station, which minimizes computation; and depending only on Γ_{max}, which minimizes storage.

This modeling approach can be extended to cases of a partially rolled-up tip vortex, or a dual-peak circulation distribution. The rollup process may not be complete by the time the tip vortex encounters the following blade. Then the strength of the tip vortex will be less than Γ_{max}, which will reduce the vortex-induced loads. It is possible to introduce a prescribed rollup, such that the tip vortex has only a fraction of the maximum strength when it encounters the following blade.

8

The remainder of the trailed vorticity outboard of the peak is still in the inboard wake, so the inboard sheet has both positive and negative trailed vorticity, divided at a radial station that corresponds to the peak. At least two sheet panels are needed to model the inboard wake, so the complete model (including the tip vortex) requires five line segments at each azimuth station.

Consider the dual-peak case, when there are two peaks of opposite sign (inboard peak Γ_I and outboard peak Γ_O) in the radial distribution of the bound circulation. Typically such loading occurs on the advancing tip at high speed, with Γ_O negative. It is assumed that there is only one zero crossing of the circulation strength between the root and the tip. It is assumed that the trailed vorticity outboard of Γ_O rolls up into the tip vortex, with strength equal to the outboard peak Γ_O. The inboard sheet has then both positive and negative trailed vorticity, divided at a radial station corresponding to the inboard peak. At least two panels are needed to model this inboard sheet. The positive trailed vorticity (generated between the two peaks) may partially roll up as well, which can be modeled by using a line segment with a physically-meaningful core radius.

The more detail that is introduced in these models of the rollup process, the more the lack of a calculation is felt. More detail usually means more empirical parameters to describe the structure. It is hardly worth the effort to model the partially rolled-up wake, since there is seldom enough information to select the modeling parameters, and the input value of the core radius will compensate for any errors in the tip vortex strength. The dual-peak model is important however, since if a single-peak model is applied to the dual-peak circulation distribution it can actually result in the wrong sign of the tip vortex strength. It is also necessary to be concerned about cases with two or more zero crossings the radial distribution of Γ; local minima and maxima in Γ from bvi; and rapid changes of Γ with azimuth. Such cases need a calculation of the rollup, not an empirical model.

2.6. Free Wake Geometry

The rotor wake geometry is important when there are close blade-vortex interactions, since the induced loading is very sensitive to the separation between the blades and tip vortices. Hence it is necessary to consider the self-induced distortion of the wake, particularly the tip vortices.

The distorted wake geometry exhibits an overall pattern in which the edges of the wake arising from the rotor disk rollup to form vortices, as behind a circular wing (figure 1). In fact this wake consists of the helical tip vortices from individual blades. The consequence of this pattern is that near the rotor the tip vortices tend to move upward on the left and right (advancing and retreating) sides of the disk, and tend to move downward in the middle of the disk. Generally then the self-induced distortion moves the tip vortices closer to the blades on the advancing and retreating sides (compared to a rigid geometry), thereby increasing the bvi loads.

The free wake geometry has a large influence on the blade airloading at low speed (advance ratios below about 0.20-0.25). At higher speeds, the propelling rotor has a large tip-path-plane angle-of-attack, typically 5-8 deg forward to provide the propulsive force. In such flight conditions the wake is convected downward relative to the disk by the normal component of the free stream, and the distorted geometry is less important.

Calculating the free wake geometry requires evaluating the induced velocity at node points in the wake. The models and methods used are similar to those for calculating the induced velocity at the rotor blade, but here the velocity is needed for points throughout the flow field, hence at an order of magnitude more points than the collocation points on the rotor disk. Much more attention to efficiency is therefore required for the free wake problem. Indeed, it is only with the development of special procedures that free wake solutions are practical for routine use in airloads calculations. A couple good, practical wake geometry analyses are available for forward flight.

2.7. Blade-Vortex Interaction

The airloads produced by blade-vortex interaction (bvi) depend on numerous physical effects, including the extent of the tip vortex rollup; the tip vortex strength; the size of the viscous core; the distorted wake geometry; lifting-surface effects on the induced loading; and possibly even vortex bursting, vortex-induced stall on the blade, or blade-induced geometry changes.

2.7.1. Tip vortex induced velocity. The viscous core of a line vortex plays a fundamental role in determining the velocity near the vortex. Consider the tangential or circumferential velocity v about a line vortex, at a distance r from the line. The core radius r_c is defined as the distance r at which the maximum value of v is encountered. For a potential line vortex (no core), $v = \Gamma/2\pi r$, where the strength Γ is some fraction of the maximum bound circulation, as determined by the rollup process. For small r, viscosity reduces the magnitude of v, by spreading the vorticity over a nonzero domain instead of a line. A Rankine vortex core produces solid body rotation of the fluid inside r_c, by having a uniform vorticity distribution concentrated entirely within the core radius. The maximum tangential velocity with a Rankine core is $v_{max} = \Gamma/2\pi r_c$. For a distributed vorticity core, one possibility has the circulation proportional to $r^2/(r^2+r_c^2)$, so half the vorticity is outside the core radius. With this core the maximum tangential velocity is $v_{max} = \Gamma/4\pi r_c$. Measurements of the velocity distributions about tip

9

vortices show that the maximum tangential velocity is much less than $\Gamma/2\pi r_c$, indicating that a substantial fraction of the vorticity is outside the core radius. Hence the distributed core model is more realistic.

The vortex-induced loads depend on the normal velocity at the wing surface, produced by a vortex at a distance h above or below the wing. For a potential vortex (no core) the maximum normal velocity (peak velocity) is $\Gamma/4\pi h$. For h = 0 (the extreme case), the peak velocity equals the maximum tangential velocity, which depends on the core type and r_c as described above. For nonzero separation distance, the Rankine core gives a peak velocity equal to the potential value when h is greater than $r_c/\sqrt{2}$, while the distributed core gives a peak velocity that is always less than the potential value. In general, the peak velocity is proportional to Γ/r_c and a function of h/r_c, so the core size is a critical parameter of the model, controlling the peak loads. For h = 0 the peak velocity of a distributed core is 50% that of the Rankine core; for h = r_c, the ratio is 70.7%. Hence using the proper core model is important for accurate prediction of the airloads.

2.7.2. Lifting-surface effects on vortex-induced loads. In close blade-vortex encounters, the induced loading varies rapidly along the span. First-order lifting-line theory will overpredict such loading, especially if the radial and azimuthal resolution in the wake is not small enough. Second-order lifting-line theory or lifting-surface theory is needed for accurate prediction of bvi loads (as well as the airloading for swept tips, yawed flow, and low aspect-ratio blades). It is found that lifting-surface effects reduce the peak induced loading by 20-40% for a vortex-blade separation equal to 25% of the chord (for various interaction angles). This effect can be approximated by increasing the viscous core size by about 15% chord.

2.7.3. Vortex-induced airloads. The peak-to-peak value of the vortex-induced loading dominates the measured and calculated blade airloads. Consider what factors influence the peak-to-peak loading.

a) Physical factors.

i) The rollup process, at the generating wing and in the wake. This process produces the strength and core size of the tip vortex at the encounter with a following blade. The strength will be less than or equal to the peak bound circulation, and the core size is typically 10-20% of the chord. If it is assumed that the strength equals the peak bound circulation when in fact the strength is less (e.g. with incomplete rollup by the time the vortex reaches the following blade), then the analysis will overpredict the loading.
ii) Lifting-surface effects, from the low effective aspect-ratio of a close interaction. If such effects are ignore, as with first-order lifting-line theory, then the analysis will overpredict the loading.
iii) Possibly vortex bursting, vortex-induced stall on the blade, local distortion of the vortex geometry by the blade, compressibility and viscous effects in general.

b) Computational factors.

i) Wake geometry. If the calculated blade-vortex separation is too large, as when a rigid wake geometry is used, then the analysis will underpredict the loading.
ii) Radial and azimuthal discretization in the wake. Typically the radial and especially the azimuthal resolution in the discretized wake are too large for close bvi. In such cases the analysis will overpredict the loading.
iii) Spanwise and timewise discretization of the loading. Typically the azimuthal resolution of the calculated airloads is too large. In such cases the analysis will underpredict the loading.

c) Measurement factors.

i) Unsteadiness and noise in the data. If the azimuthal angle of the bvi changes from revolution to revolution, then the averaging process will reduce the measured peak loads, and the analysis will overpredict the loading.

The core size r_c is a convenient parameter with which to control the amplitude of the calculated bvi loads, since it determines the maximum tangential velocity about the vortex (always inversely proportional to r_c). Moreover, the core size is seldom either measured or calculated, so it is an input parameter of the analysis. The approach thus is to model all effects possible in the theory, as accurately as possible; and then use the value of r_c to account for not only the actual viscous core radius, but also all phenomena of the interaction that are not otherwise modelled (or are inaccurately modelled). A goal for the development of better models is that the vortex core size represent the actual physical core (10-20% chord) and nothing else.

3. CALCULATIONS AND CORRELATION

This section summarizes results from calculations and correlation of helicopter rotor behavior, particularly flapping, airloads, and power. The low speed results cover the influence of nonuniform inflow and wake geometry; the modeling of blade-vortex interaction, including the influence of the wing model and core size; and inboard bvi. The high speed results cover the influence of nonuniform inflow and wake geometry; the influence of the dual-peak model and inboard rollup; the influence of the wing model; modeling of swept tips; and the blade section moment. Finally the wake rollup model is

discussed. Again, the results summarized are from the author's experience. Details of the calculations and correlation are given in references 3, 5-9.

3.1. Low Speed Results

3.1.1. Nonuniform inflow and free wake geometry.

The wake geometry has an important role at low speeds (figure 1). Lateral flapping in low speed forward flight is a sensitive measure of the effects of the rotor wake. The lateral tip-path-plane tilt of an articulated rotor depends primarily on the longitudinal gradient of the induced velocity distribution over the disk. The induced velocity in forward flight is larger at the rear of the disk than at the front, which produces larger loads at the front, hence an aerodynamic pitch moment on the rotor. An articulated rotor responds to this moment like a gyro, and so the tip-path-plane tilts laterally, toward the advancing side (in forward flight there is also a small lateral flapping contribution proportional to the coning angle). The lateral flapping is underpredicted when uniform inflow is used, and even when nonuniform inflow based on a rigid, undistorted wake geometry is used. Below advance ratios of about 0.16, its is necessary to include the calculated free wake in order to obtain a good estimate of the lateral flapping. The self-induced distortion of the tip vortices leads to numerous instances of bvi in which the vertical separation is a small fraction of the blade chord. The resulting bvi-induced velocity has a large once-per-revolution content, equivalent to a longitudinal gradient of the induced velocity, which produces the observed lateral flapping.

Low speed airloads exhibit significant blade-vortex interaction. The free wake geometry must be used in order to accurately calculate the bvi loads at low speed. The free wake geometry is also needed to calculate rotor power for advance ratios below about 0.20, where a rigid geometry produces an increasing underprediction of the induced power. Using a nonuniform inflow and free wake geometry calculation, good correlation can be obtained with flight test measurements of the performance for $\mu = 0.15$-0.25, which covers the crucial minimum power point. The correlation at lower speeds is particularly sensitive to the accuracy of the free wake geometry.

3.1.2. Blade-vortex interaction.

At low speed, the free wake geometry places the tip vortices so close to the blades that the calculated flapping and airloads are sensitive to the details of the bvi calculation, particularly accounting for lifting-surface effects and the value of the tip vortex core radius (which determines the maximum velocity induced by the vortex). Comparisons can be made between second-order lifting-line theory, a lifting-surface theory correction, and simply using a larger effective core size. For each model, the core size needed for good correlation can be determined, and compared with the expected value of the physical viscous core.

For correlations of both lateral flapping and low speed airloads, the second-order lifting-line theory gives best results, especially at very low μ. Second-order lifting-line theory and a lifting-surface theory correction require about the same core size. For the airloading at the blade tip, the best core size is 21-23% chord, which is at the high end of the expected range of physical viscous core sizes. This result is based on correlations for two rotors. The correlation of tip airloading suggests that the core size varies with azimuth, being larger for tip vortices created on the retreating side. The first-order lifting-line theory requires a core increase of about 15% chord in order to simulate lifting-surface effects on the bvi loads.

At very low speeds, bvi can be encountered that is so strong it produces negative lift at azimuth angles around 75 deg. This calculated phenomenon can occur even at $\mu = 0.20$ for some rotors. At very low speeds (μ below about 0.10) there has been little airloads correlation however, and the performance results suggest that the calculated free wake geometry is producing too much bvi. Moreover, the models of the wake rollup process outlined above do not consider such loading.

Because there is so much bvi at low speed (up to $\mu = 0.20$ for some rotors), there is a significant influence of the core size on performance. A larger core radius decreases the induced power, as expected since it reduces the magnitude of the nonuniform variations of inflow. There is also a significant influence of second-order vs first-order lifting-line theory, with the latter reducing the calculated induced power (which will be further reduced by the larger core size that first-order lifting-line theory needs to simulate lifting-surface effects on the bvi loads).

3.1.3. Inboard blade-vortex interaction.

It has been observed that when vortex-induced loads are calculated using the core size that gives good correlation at the blade tip, the strength of the bvi is significantly overpredicted for inboard radial stations. An examination of measured low speed airloads indicates that the vortex-induced loading is high when the blade first encounters the vortex, on the advancing side; decreases inboard as the blade sweeps over the vortex, on the front of the disk; and the recovers again on the retreating side. The core size can be increased for collocation points on the inboard part of the blade in order to eliminate (but not explain) this problem.

Evidently there is some phenomenon limiting the loads. Among the possibilities that have been proposed are the following.

a) Local local distortion of the vortex geometry.
b) Bursting of the vortex core, induced by the blade. The bursting must propagate upstream in order to affect the bvi loading, but must not propagate too far.

c) Interaction of the vortex with the trailed wake it induces behind the blade, with the effect of diffusing and reducing the circulation in the vortex.

d) Local flow separation produced by high radial pressure gradients on the blade. This is an unsteady separation, introducing delays needed to reduce the bvi only on the inboard part of the blade.

e) Viscous effects on the interaction, because the blade-vortex separation is much smaller on the front of the disk than on the sides.

Note that (b), (c), and (d) do not provide a mechanism for the bvi loads to recover on the retreating side; and that (b) and (c) would also affect subsequent bvi of the vortex element.

An examination of the calculated free wake geometry at low speed suggests possibility (e) as a cause of the suppression of the vortex-induced loads on the inboard part of the blade, i.e. on the front of the disk. The tip vortex is typically above the following blade throughout the interaction. On the advancing and retreating sides it is perhaps 4% R above the blade tips, but on the front of the disk (where the induced loads are suppressed) the vortex is much closer to the blade. It is postulated that this closer interaction may involve viscous phenomena that are responsible for reducing the loads, while the interaction on the advancing and retreating sides is well calculated by inviscid wing theory.

Increasing the core size for inboard collocation points is a simple way to model the effects on the airloads, but no explanation of the physics is intended. The exact physical mechanism involved remains speculative. More detailed measurements of the aerodynamics, including the wake geometry, are needed to explore this phenomenon.

3.2. High Speed Airloads

3.2.1. Nonuniform inflow and free wake geometry. Correlation of both airloads and power show that the free wake geometry is less important at high speed, but that nonuniform inflow is still needed. Nonuniform inflow increases the induced power and decreases the profile power at high speed, compared to calculations based on uniform inflow. Typically there is a net increase in the total power with nonuniform inflow, but even if the only influence were to change the distribution between induced and profile losses, the implications for design optimization would be significant. The ratio of the induced power to the ideal power (from momentum theory) is typically about 3.0 at high speed. This large increase in induced power is a consequence of the reduced effective span of the rotor disk under the loading distribution of forward flight. Since the lifting capability of the retreating side of the disk is limited by low velocities and airfoil stall, and the lifting capability of the advancing side by the requirement of roll-moment balance with a flapping rotor, the working part of the rotor disk is restricted to the front and back at high speeds. The factor of 3.0 in induced power implies an effective span equal to 58% of the rotor disk diameter.

3.2.2. Dual-peak model and inboard rollup. The blade loading in high speed is often negative on the advancing tip, as a consequence of flap moment equilibrium. Hence it is necessary to model the wake created by a dual-peak span loading (inboard and outboard peaks of opposite sign), optionally with multiple rollup of the trailers. Three wake models can be examined:

a) A single-peak model, using the maximum bound circulation. When the tip loading is negative, this model has both the sign and magnitude of the tip vortex strength wrong.

b) A single-peak model, using the outboard bound circulation peak for the tip vortex strength. Applied to the dual-peak loading case, this model has the wrong distribution of trailed vorticity for the inboard sheet.

c) A dual-peak model. For the dual-peak loading case, this model has a different structure of the inboard wake than (b), and in addition changes in the loading can feed into the tip vortex strength and increase the differences between the two models.

The calculated airloads show a significant effect of the dual-peak model. It is essential to get the correct sign of the tip vortex, so model (a) is not good. Sometimes the loading is dominated by the tip vortex, while sometimes the inboard wake structure is also important (so model (c) above is best). Sometimes rollup of the inboard trailed wake changes the airloading, and sometimes not. The dual-peak model has a modest influence on the calculated power, decreasing the induced power some.

3.2.3. Wing model and aerodynamic corrections. The calculated airloads in high speed show some influence of second-order vs first-order lifting-line theory. Since the magnitude of yawed flow increases with advance ratio, it is expected that second-order lifting-line theory will be needed. The power also shows an influence of the wing model, with first-order lifting-line theory decreasing the induced power and increasing the profile power. The aerodynamic corrections for sweep will reduce the profile power for a blade with a swept tip. The radial drag increases the profile power. At high thrust, the yawed and swept flow corrections to angle-of-attack are also important.

3.2.4. Swept tips. Swept tips have proven beneficial to both the performance and structural loads of rotor blades, and are found on several production helicopters. These benefits are produced by a combination of aerodynamic and dynamic effects, in the unsteady and compressible aerodynamic environment of the rotor blades. Key features of an analysis applied to swept-tip rotor blades include:

12

a) Second-order lifting-line theory. The lifting-line (bound vortex) is at the quarter-chord, following the swept span line, with the induced velocity collocation point at the three-quarter-chord. Note that a first-order lifting-line theory (collocation point at quarter-chord) can not consistently use a swept lifting-line (and to do so produces unreasonable effects).

b) The section Mach number used is that normal to the swept quarter-chord line. In addition, there are swept and yawed-flow corrections for the angle-of-attack, which primarily affect the stall and drag of the blade section.

For a rotor blade with a highly swept tip (e.g. 27 deg at 95% R and larger outboard), good correlation is obtained with the measured tip airloading at high speed. Particularly important are the use of second-order lifting-line theory, and the Mach number normal to the swept quarter-chord. The Mach number correction on the swept tip can be enough to keep the effective Mach number less than the critical value over most of the rotor disk.

3.2.5. Blade section moment. High speed airloads calculations show good correlation with measured section moments at 92% R. It should be noted that in the absence of major effects of stall and compressibility on the loading, the principal contributor to the section moment is the unsteady noncirculatory term. Correlation of the section moment deteriorates outboard of 92% R however. The measured section moment varies significantly with radial station at the tip, but the calculated moments show little variation. The calculated angle-of-attack varies along the tip span, but typically the resulting static moment coefficient does not change much. Moreover the pitch rate does not change much radially at the tip, so the unsteady term does not change either. What is missing in the calculation is the effect of the chordwise induced velocity gradient on the section moment.

These results reflect the limitation of the aerodynamic model: the lifting-line theory is second-order for lift but only first-order for moment, so the best accuracy for pitch moments is expected on the inboard part of the blade. The pitch moments have an important influence on even the lift and performance of a rotor, since the blades generally have significant elastic torsion motion in response to the aerodynamic moments. Hence second-order accuracy is needed for the pitch moments as well as for the lift.

3.3. Wake Rollup Model.

An examination of the calculated spanwise distribution of bound circulation allows an assessment of the assumptions behind the wake rollup model. At low speed, the influence of bvi is observed, and sometimes the effects of nonlinear twist. At very low speed, the bvi can be so strong it produces negative lift over a narrow range of azimuth angle around 75 deg. At high speed, the influence of reverse flow is observed, and often negative loading on the advancing tip.

In general, the calculated spanwise distribution of Γ is frequently found to be quite different than assumed in developing the wake models. Often the peak in the loading is very far inboard rather than near the tip, especially on the advancing side. Often there are rapid changes in the sign of Γ, both azimuthally and radially.

A general conclusion of airloads correlation investigations is that more must be known about the distorted wake geometry, tip vortex formation, and wake rollup. Measurements are needed of the wake geometry and rollup, and the induced velocity. Such measurements are difficult to make (see refs. 12-13), although there are promising new techniques such as the wide-field shadowgraphs (ref. 14). Velocity measurements are difficult because point measurements take a long time to cover the flow field, and traverses through the rotor wake are very sensitive to unsteadiness and to small changes in the geometry. Moreover, the induced velocity that appears in the wing theories is not a quantity that can be measured. Specific measurements needed include:

a) The self-induced distortion of the entire wake, and the structure and extent of the rollup of the tip vortices and inboard wake.

b) From velocity measurements, the strength of the tip vortices, the core size, and the peak velocities.

Ideally these measurements should be made simultaneously with airloads and performance measurements.

4. AERODYNAMIC AND WAKE MODELS FOR AEROELASTICITY

This section describes two-dimensional and rotary wing unsteady airloads theories, including dynamic inflow models. The inner problem of lifting-line theory needs the noncirculatory airloads: the unsteady lift and moment, without static terms or shed wake effects. For linear stability and response solutions, an ordinary-differential-equation form of the wake model is needed (usually with simplifications).

4.1. Two-Dimensional Unsteady Airloads

4.1.1. Two-dimensional unsteady thin airfoil (Theodorsen theory).

Unsteady motion of an airfoil produces a shed wake because of the variation of the bound circulation with time. This wake vorticity produces an induced velocity at the airfoil that tends to cancel the lift, i.e. the shed wake produces a feedback reducing the circulatory lift. In addition there are noncirculatory lift and moment terms, independent of the wake effects, including rate (damping) and acceleration (virtual mass) effects.

For purely harmonic motion at frequency ω, the two-dimensional lift is $L = C \, L_Q + L_{NC}$, where L_Q is the quasistatic lift, from the angle of attack at the three-quarter-chord; L_{NC} is the noncirculatory lift; $C(k)$ is the lift-deficiency function; and $k = \omega b/U$ is the reduced frequency. For the section moment, the theoretical aerodynamic center is at the quarter-chord; and there is a noncirculatory pitch damping moment from the lift at the three-quarter-chord (hence zero for pitch about an axis at the three-quarter-chord).

Care is required in translating the description of the motion in the two-dimensional airfoil theory to the parameters of a rotor blade. Note that the aerodynamic theory is based on boundary conditions involving the velocity normal to the chord, in Theodorsen's theory consisting of a uniform term plus a linear variation over the chord. The key to identifying the corresponding quantities in the rotor analysis is to distinguish between angle-of-attack (velocity) and pitch rate (velocity gradient). For example, translating from the Theodorsen definition of the motion (angle of attack α and heave h, with free stream velocity U) to the motion of a rotor blade in hover gives:

Theodorsen		helicopter		hover pitch/flap
$U\alpha + \dot{h}$	$=$	$u_T\theta - u_P$	$=$	$r(\Omega\theta - \dot{\beta})$
$\dot{\alpha}$	$=$			$\dot{\theta} + \Omega\beta$

where θ and β are the pitch and flap angles of an articulated rotor.

The effect of the shed wake on the loads is contained in the Theodorsen lift-deficiency function $C(k)$. At zero frequency, $C = 1$, while at high frequency C approaches $1/2$, so the wake reduces the circulatory lift. There is also a moderate phase lag, which can change aerodynamic springs into damping forces. The reduced frequency for a rotor blades is approximately

$$k = \omega b/U = (n\Omega)(c/2)/(\Omega r) = nc/2r \approx 0.05n$$

for harmonic motion at n/rev. Hence k is small for the lower harmonics (in particular the quasistatic assumption is reasonable for 1/rev loading), but significant for higher harmonics.

4.1.2. Noncirculatory loads.

The rotary wing aerodynamic model requires from unsteady airfoil theory the noncirculatory loads, since the shed wake effects are accounted for through the induced velocity not the lift-deficiency function, and the static loads are obtained from airfoil tables. The noncirculatory terms are essential for the aerodynamic pitch damping, and are sometimes needed for the lift and even the virtual mass terms. Excluding the static terms (from the angle-of-attack at the quarter-chord) and the shed wake (i.e. setting the lift-deficiency function $C = 1$), the noncirculatory lift and moment are:

$$L_{US} = \rho \, 2\pi \frac{c^2}{8} \left(2UB + \dot{w}_{QC} + \dot{B} \, \frac{c}{4} \right)$$

$$M_{US} = -\rho \, 2\pi \frac{c^3}{32} \left(UB + \dot{w}_{QC} + \dot{B} \, \frac{3}{8} \frac{c}{} \right)$$

where L is the lift and M the moment about the quarter-chord; c the chord and U the section velocity; w_{QC} is the upwash velocity seen by the blade at the quarter-chord ($U\alpha + \dot{h}$); and $B = dw/dx$ is the gradient of the downwash along the chord ($\dot{\alpha}$). These equations include the effect of a time-varying free stream, but do not account for reverse flow.

4.1.3. Two-dimensional unsteady airfoil theory for rotors.

For the rotary wing it is necessary to consider a time-varying free stream, since the section velocity U has a periodic (1/rev) variation in forward flight. For the noncirculatory terms it is only necessary to include the derivatives of U in the results. The effect of the time-varying free stream on the lift-deficiency function is more complicated, since it produces stretching and compressing of the shed wake. An approximation for low frequency variation of U is to simply use the Theodorsen function $C(k)$, with the reduced frequency calculated from the local

value of U. In addition there will be interharmonic coupling, between the harmonics of the lift and the harmonics of the motion.

A two-dimensional model can be developed as an approximation for a hovering rotor (Loewy's theory). The rotor wake in hover consists of helical sheets below the rotor disk. With unsteady motion, there is shed vorticity in the spirals. This returning shed wake can have a significant influence on the loading when the wake is close to the disk, i.e. at low thrust in hover. The wake configuration near the blades can be approximated by planar sheets parallel to the disk plane. Hence a two-dimensional model introduces the returning shed wake as vortex sheets arrayed below the airfoil.

The only effect of these returning wake sheets on Theodorsen's theory is to replace the lift-deficiency function with Loewy's function: $C'(k, \omega/\Omega, h/b)$, where h/b is the wake spacing and ω/Ω gives the relative phase of the vorticity in successive sheets (only the fractional part is important). For harmonic oscillation, ω/Ω = integer, the vorticity in all the sheets is exactly in phase, and capable of producing large effects on the loads. (For a multi-bladed rotor it is necessary to relate the wake from the various blades, typically by using multiblade coordinates for the motion. The result is equivalent to a single blade for harmonic oscillations or the collective modes.)

The behavior of C' at low k is of most interest for rotors. If ω/Ω is not an integer, the returning shed wake just produces order k (small) corrections to the Theodorsen function. For harmonic oscillations, ω/Ω = integer, major changes to the behavior of C' are obtained; specifically, for low reduced frequency

$$C' \cong \frac{1}{1 + \pi b/h} = \frac{1}{1 + \pi\sigma/4\lambda}$$

where an estimate of the wake spacing from vertical convection of the wake by the mean induced velocity λ gives $h/b = 4\lambda/\sigma$. This is a good estimate for C' even up to k about 0.5, but note that it suggests that $C' \neq 1$ at k = 0 (i.e. it is not a proper limit for k = 0, and should only be used for small but nonzero k). Typically λ = 0.05-0.07 gives h/b = 3-4, and so roughly C' = 0.5. Hence a substantial reduction of the unsteady loads is possible, because all the vorticity is in phase. The case of harmonic oscillation includes cyclic pitch control (1/rev), and flutter or vibration of a blade with a natural frequency at n/rev.

4.2. Rotor Unsteady Aerodynamic Models

The theories of Theodorsen and Loewy provide guidance for unsteady aerodynamic model of rotors, but are not sufficient themselves for most applications. A result for harmonic motion is not appropriate, since a time domain model is needed for most solution procedures (even for the periodic solution in trim). The actual geometry of the wake must be considered, including perturbations of the geometry because of the unsteady motion. The unsteady trailed wake must be considered, as well as the shed wake.

Early work on rotor unsteady aerodynamic models included unsteady vortex theory and perturbation momentum theory. Developing rotor models is difficult because of the complex structure of the wake. Unsteady vortex theory uses the actuator disk model, which provides major simplifications: continuous rather than discrete distribution of vorticity in the wake, and constant coefficient models for dynamics. Perturbation momentum theory provides simple results (which can also be derived from unsteady vortex theory).

4.3. Dynamic Inflow

Finite state models represent the current state-of-the-art for rotor unsteady aerodynamic theory (the wake effects). Dynamic inflow relates parameters defining the induced velocity and aerodynamic loads on the rotor disk, by means of ordinary-differential equations (ODE), usually from a simplified model of the rotor. An ODE representation of the wake effects is ideal for use in stability calculations.

The lowest order dynamic inflow theory represents the wake-induced velocity perturbation by terms giving uniform and linear variation over the disk:

$$\delta\lambda = \lambda_u + \lambda_x r \cos\psi + \lambda_y r \sin\psi$$

$$\lambda = (\lambda_u \quad \lambda_x \quad \lambda_y)^T$$

and represents the unsteady loading by the perturbation aerodynamic thrust and hub moments:

$$L = (\delta C_T \quad -\delta C_{My} \quad \delta C_{Mx})^T$$

Then λ is obtained from L by a first order differential equation:

$$\tau \, \dot{\lambda} + \lambda = (\partial \lambda / \partial L) \, L$$

It is also necessary to consider the induced velocity perturbations produced by rotor inplane- and vertical-velocity changes. This is a low order, global model of the rotor unsteady aerodynamics, representing low frequency effects. Note that a differential equation implies a lift-deficiency function C that is a ratio of polynomials, which is never the correct form for a finite-order model.

With no flap hinge offset a rotor can not sustain a hub moment, so the low frequency aerodynamic moments will be small; hence the linear inflow terms are particularly important for hingeless rotors. The static derivative matrix $(\partial \lambda / \partial L)$ can be obtained from differential momentum theory (which gives good results for hover), from unsteady actuator disk theory (which is needed for good results in forward flight), or identified from experimental rotor response data. Typically the time lag is written $\tau = \kappa (\partial \lambda / \partial L)$, where κ is a constant and diagonal matrix. The terms in κ can be obtained from the apparent mass of an impermeable disk subject to linear or angular motion; the resulting values are supported by experimental data.

Omitting the time lag produces a quasistatic model, the effects of which are given by a constant lift-deficiency function C'. If the dominant aerodynamic forces are lift perturbations caused by angle-of-attack changes, then the aerodynamic influence is described by a blade Lock number γ (which contains the lift-curve-slope). In this case the effects of the quasistatic dynamic inflow model are largely represented by an effective Lock number: $\gamma^* = C' \gamma$. However, frequently the time lag is needed to properly represent the effects of the unsteady aerodynamics.

Many investigations have examined the influence of dynamic inflow. It is found that unsteady aerodynamic are important for most rotor aeroelastic problems. It is only the complexity of the models required that prevents unsteady aerodynamics from always being included in rotor analyses.

5. AIRLOADS AND STRUCTURAL DYNAMICS

This section presents the elements of rotor and airframe structural dynamics, and discusses coupled aerodynamic-wake-motion solutions for the trim problem. Finally, comprehensive airload prediction programs are discussed, with an assessment of the technology they incorporate.

5.1. Influence of Blade Structural Dynamics on Airloads

Rotor airloads calculation is an aeroelastic problem. Consider the aerodynamic environment of a rotor in forward flight. The helicopter flies with the rotor nearly horizontal, with a small angle-of-attack of the disk to produce the needed propulsive force from tilt of the rotor thrust vector. With an inplane component of the forward speed, the aerodynamic environment in forward flight is no longer axisymmetric, as for hover. The velocity seen by the blades is higher on the advancing side and lower on the retreating side. This basic 1/rev variation in the aerodynamic environment means that the loading and resulting response of the blades will be periodic in forward flight.

If the rotor blades were operated at a constant angle-of-attack around the azimuth, the 1/rev variation of velocity would produce a rolling moment. A rolling moment from the rotor means that the aircraft must fly with a roll angle (or crash), and that there will be unacceptable 1/rev structural loads on the root of the blade. The design solution is to allow blade motion, so the loads are countered by aerodynamic forces rather than by structural reactions at the root. So in forward flight the rotor blade has at least a 1/rev out-of-plane (flap) motion. The conventional design (the articulated rotor) has a flap hinge at the root, hence no structural moment at all at the hinge. A hingeless rotor has enough flexibility at the root to allow similar motion. The flap motion produces inplane loads, so lag motion must be allowed as well. Pitch motion is required to control the blade, and there will be control system and blade torsion flexibility that allow elastic torsion motion.

These conclusions are elementary. The point is that the fundamental design approach for rotors implies a time-varying (periodic) motion even in steady flight, and that large structural and inertial forces are associated with the rigid body and elastic motion of the blades. Hence rotor airloads calculation is an aeroelastic problem.

An examination of the influence of structural dynamics on calculated airloads shows that in general the effects of elastic blade motion are comparable to those of the various wake modeling features. Elastic torsion motion directly changes the blade angle-of-attack, and so has a significant effect on the airloads. The section velocity changes produced by elastic and higher harmonic flap/lag motion are less important. Elastic torsion motion can have a magnitude from 1 to 10 deg, with mean, 1/rev, and higher harmonic terms. Note that the mean and 1/rev elastic motion of the blade pitch because of control system flexibility will not change the airloads for a specified trim thrust and propulsive force (these motions show up in the position of the controls needed to achieve the specified trim condition). The elastic torsion motion of a blade can be large because of a large aerodynamic pitch moment, or low torsional stiffness of the blade; and in response to aerodynamic and

inertial forces on a swept tip; and sometimes because of chordwise offset of the blade center-of-gravity and aerodynamic-center, or resonant coupling with bending.

5.2. Elements of Rotor and Airframe Structural Dynamics

5.2.1. Rotor blade structural dynamics. Equilibrium of the inertial (including centrifugal and Coriolis for rotating blades), structural, aerodynamic, and gravitational forces on a component produces partial-differential equations (PDE) for the rotor blade. These PDE have as independent variables the three space coordinates and time, and as dependent variables the deflected position of the component.

Rotor blades have a high aspect-ratio of the structural elements, which allows engineering beam theory to be used. The equations are still PDE, but beam theory reduces the spatial dependency to a single dimension: the independent variables are blade span and time, and the dependent variables are flap/lag bending, axial extension, and torsion of the beam. Nonlinear structural and inertial effects are important for rotors, as well as body (gravity) and surface (aerodynamic) forces. Hence beam theories for rotor blades have required considerable development.

As an example, consider the out-of-plane bending of a rotor blade. Let $z(r)$ be the out-of-plane deflection. The PDE for bending is:

$$(EI\,z'')'' - \left(\int_r^R m\Omega^2\rho\,d\rho\,z'\right)' + m\ddot{z} = L$$

where EI is the section stiffness, m is the section mass, and L is the aerodynamic section lift force. Appropriate boundary conditions for a free tip and a hinged or cantilever root are required to complete the problem definition.

The next step in solving the structural dynamic equations is to discretize the spatial dependence, changing the PDE into ordinary-differential equations (ODE) in time for generalized coordinates. Various methods are used to perform the spatial discretization: modes, transfer matrices, finite differences, and finite elements. In the modal approach, the deflection is expanded in the radial mode shapes; it is important to choose the modes so that a small number will describe the motion well.

In the example of out-of-plane bending, a good choice is the modes obtained from free vibration of the rotating blade at frequency v. The modal equation produced has a series of solutions $\eta_k(r)$ with eigenvalues v_k, such that the modes are orthogonal when weighted by the section mass m. The deflection is expanded as a series in the modes:

$$z(r,t) = \sum_{k=1}^{\infty} \eta_k(r)\,q_k(t)$$

with generalized coordinates q_k. Substitute this expansion into the PDE for bending, use the modal equation, multiply by η_i and integrate over the blade, and use orthogonality in order to obtain the ODE for q_k:

$$I_k(\ddot{q}_k + v_k^2 q_k) = \int_0^R \eta_k L\,dr$$

The section lift can be obtained from airfoil tables:

$$L \cong \frac{1}{2}\rho U^2 c\, c_\ell(\alpha, M)$$

with the angle-of-attack and Mach number

$$\alpha = \theta - \tan^{-1}u_P/u_T$$

$$M = U/c_s$$

$$u_P = \Omega R\lambda + \dot{z} + z'\,u_R$$

So even for the simple problem of out-of-plane bending and quasistatic aerodynamics, the aerodynamic forces couple the modes, introduces nonlinearities, and produces time variation of the dynamic equation.

17

In general, the structural dynamic terms are not diagonal even for simple cases. The problem consists of coupled equations for generalized coordinates q representing the bending, torsion, and axial motion of the blade:

$$M(\ddot{q}, q, t)\, \ddot{q} \ + \ K(\dot{q}, q, t) \ = \ F$$

These are quite complicated equations: nonlinear because of the structural and inertial forces (left-hand-side) and aerodynamic forces (right-hand-side), and time-varying because of the forward flight aerodynamics and the rotating/nonrotating frame interfaces.

5.2.2. *Structural dynamic problems.* For aeroelastic stability and response calculations (flutter), linearized equations are required, in both the structural dynamic and aerodynamic terms.

Calculation of the rotor structural loads requires a solution for the nonlinear response, and demands much attention to the aerodynamics. It is necessary to consider the structural, inertial, and aerodynamic forces on the rotor, and even on the entire helicopter. Feedback of the hub motion (produced by the rotor hub loads) to the rotor can change the calculated hub loads by 20% or more.

Vibration is the oscillatory response of the helicopter airframe to the rotor hub reactions. Periodic excitation of the helicopter can also occur from the rotor wake acting on the airframe. Vibration calculation adds increased importance of the airframe structural dynamics and rotor/airframe aerodynamic interference to what is required for the structural loads calculations. The airframe response is periodic in steady flight, with components primarily at 1/rev and N/rev (where N is the number of blades). The vibration is low in hover, and increases with speed or thrust to a high level, because of the effects of stall and compressibility on the rotor. Vibration is also high in transition (low speed), and descending or decelerating flight, because of wake effects on the blade loading (blade-vortex interaction).

5.3. Coupled Aerodynamic/Wake/Motion Solutions

5.3.1. *Trim solution.* Trim refers to a steady state, unaccelerated flight condition, for which the rotor and airframe motion are periodic (ignoring any oscillatory interaction between a main rotor and a tail rotor). Usually the inverse problem is to be solved: determine the control required for a specified flight condition. The trim solution requires calculating the periodic airloading and rotor motion, and the steady trim variables. Then the performance, structural loads, noise, and other results can be evaluated.

It is the converged solution that is required, not any intermediate transients, so a strictly physical approach is not necessary. Often there are separate solutions for the periodic rotor motion and steady trim variables, since these two parts of the problem have different kinds of equations (differential equations for the periodic motion, algebraic equations for the trim variables). The equations are nonlinear, so an iterative solution procedure is needed in any case. Thus there is an inner loop in which the periodic rotor motion and airframe vibration are calculated. The solution procedure can be in the frequency or time domain. A frequency domain solution represents the motion by a Fourier series, but usually evaluates the aerodynamic loading in the time domain (since it is nonlinear, and because of the large number of aerodynamic variables). A time domain solution can be based on numerical integration to convergence, periodic shooting, or other methods. There is an outer loop in which the trim variables (rotor controls, aircraft Euler angles, etc.) required to achieve the specified trim state (free flight or wind tunnel) are evaluated. The solution method for this loop might be a modified Newton-Raphson, periodic shooting, or an autopilot.

For efficiency and to improve convergence, it is important to move computationally intensive calculations outside inner loops (if allowed by weak coupling). An important case is the calculation of the wake geometry and influence coefficients for the nonuniform inflow model, which can be moved outside the trim iteration. By making this the outermost loop, the influence coefficients are evaluated as few times as possible. The resulting efficiency is crucial to making the nonuniform inflow calculation practical for routine use. This approach is possible because the coupling between the wake geometry and the rest of the solution is relatively weak, as long as the rotor is trimmed to a specified thrust and tip-path-plane angle-of-attack.

The trim solution procedure is thus partitioned and iterative. Figure 8 illustrates one way to make the partition. Each of the boxes in figure 8 has a solution for the periodic, trim response of part of the problem. Note that the blade aerodynamics are inside the rotor box, hence are the innermost loop of the solution procedure. The reasons for this particular partition of the problem are summarized below.

loop	interface	reasons for partition
rotor/body	hub motion hub forces	interharmonic coupling from rotating/nonrotating interface
circulation	induced velocity circulation	differential vs integral equations, and large number of circulation variables
trim	controls trim quantities	inverse problem, and algebraic equations
wake geometry	influence coefficients circulation	move computationally intensive calculations outside

There are however many methods currently in use to solve the trim problem.

5.4. Comprehensive Airload Prediction Programs

Comprehensive analyses bring together the most advanced models of the geometry, structure, dynamics, and aerodynamics available, subject to the constraints of economy and accuracy. The objective is to calculate blade motion and airloading; performance and trim; blade loads, control loads, vibration, and noise; aeroelastic stability; and handling qualities and response. The calculations are to be performed with a consistent, balanced, yet high level of technology in a single tool, applicable to the entire aircraft, and a wide range of rotor and aircraft configurations. Often however the range of application is restricted, perhaps to improve efficiency, more often for historical reasons. Often the highest level of technology is still found only in restricted development tools.

In general, the term "comprehensive" implies a focus on coupling of components, interaction of disciplines, and integration of technology. Helicopter problems are inherently complex and multidisciplinary, so helicopter analyses are always being driven toward a consideration of "comprehensive" issues.

The following are typical technical limitations of comprehensive airload prediction programs, which also define the technology boundaries for research.

a) Aerodynamics: Empiricism is required in order to cover all aspects of the aerodynamics, such as wake rollup, dynamic stall, and rotor/airframe interaction. The models are usually based on lifting-line theory, and a discretized, inviscid wake.
b) Dynamics: A new rotor or helicopter configuration often requires a new development of the dynamic equations, because of a lack of flexible modeling techniques. The models are usually based on beam theory (modal or finite-element); and small to moderate (but nonlinear) deflections.
c) Solution: The solution procedures are characterized by heuristic development and a lack of robustness.
d) Software: The software is too frequently still characterized by lack of transportability and modularity, poor input and output, or inadequate documentation. The implementations often have a lack of balance between the disciplines.

Subjects receiving particular attention now in research and development include coupling of components, integration of technology, and the software.

6. CONCLUDING REMARKS

This lecture has presented fundamental considerations regarding the theory and modeling of rotary wing airloads, wakes, and aeroelasticity. The topics covered were: (a) airloads and wakes, including lifting-line theory, wake models and nonuniform inflow, free wake geometry, and blade-vortex interaction; (b) aerodynamic and wake models for aeroelasticity, including two-dimensional unsteady aerodynamics and dynamic inflow; and (c) airloads and structural dynamics, including comprehensive airload prediction programs. Results of calculations and correlations were summarized.

The distinguishing characteristic of the rotary wing for the aerodynamicist is that it is essential to consider the rotor wake and blade motion. The following are some aspects of rotary wing aerodynamics that deserve attention in future research.

a) Lifting-line theory at its best gives good results, but it has too many assumptions and approximations. Progressive development of better theories is needed.
b) The wake theory is limited by the fact that the rollup is modeled rather than calculated. A first-principles calculation of the structure and extent of wake formation is needed.
c) Blade-vortex interaction loads and free wake geometry calculations need further development.
d) There is a continuing need for detailed measurements of rotor airloads and wake properties.

REFERENCES

1) Johnson, W. Helicopter Theory. Princeton, New Jersey, Princeton University Press, 1980.

2) Johnson, W. "Development of a Comprehensive Analysis for Rotorcraft." Vertica, vol 5, no 2-3, 1981.

3) Johnson, W. "Assessment of Aerodynamic and Dynamic Models in a Comprehensive Analysis for Rotorcraft." Computers and Mathematics with Applications, vol 12A, January 1986.

4) Johnson, W. "CAMRAD/JA, A Comprehensive Analytical Model of Rotorcraft Aerodynamics and Dynamics." 1988, Johnson Aeronautics, Palo Alto, California.

5) Johnson, W. "Wake Model for Helicopter Rotors in High Speed Flight." November 1988, NASA CR 177507.

6) Johnson, W. "Calculation of Blade-Vortex Interaction Airloads on Helicopter Rotors." Journal of Aircraft, vol 26, no 5, May 1989.

7) Bousman, W.G.; Young, C.; Gilbert, N.; Toulmay, F.; Johnson, W.; and Riley, M.J. "Correlation of Puma Airloads -- Lifting-line and Wake Calculation." September 1989, European Rotorcraft Forum, Amsterdam.

8) Johnson, W. "Calculation of Airloads on a Helicopter Rotor Blade with a Swept Tip." September 1989, NASA CR 177536.

9) Johnson, W. "Rotor Wake and Aerodynamic Model Influence on Calculated Helicopter Performance." 1990, NASA CR.

10) Bousman, W.G. "The Response of Helicopter Rotors to Vibratory Airloads." November 1989, American Helicopter Society National Specialists' Meeting on Rotorcraft Dynamics, Arlington Texas.

11) Srinivasan, G.R., and McCroskey, W.J. "Navier-Stokes Calculations of Hovering Rotor Flowfields." Journal of Aircraft, vol 25, no 10, October 1988.

12) Landgrebe, A.J., and Bellinger, E.D. "An Investigation of the Quantitative Applicability of Model Helicopter Rotor Wake Patterns Obtained from a Water Tunnel." December 1971, U.S. Army Air Mobility Research and Technology Laboratories, TR 71-69.

13) Landgrebe, A.J., and Egolf, T.A. "Rotorcraft Wake Analysis for the Prediction of Induced Velocities." January 1976, U.S. Army Air Mobility Research and Technology Laboratories, TR 75-45.

14) Norman, T.R., and Light, J.S. "Application of the Wide-Field Shadowgraph Technique to Rotor Wake Visualization." October 1989, NASA TM 102222.
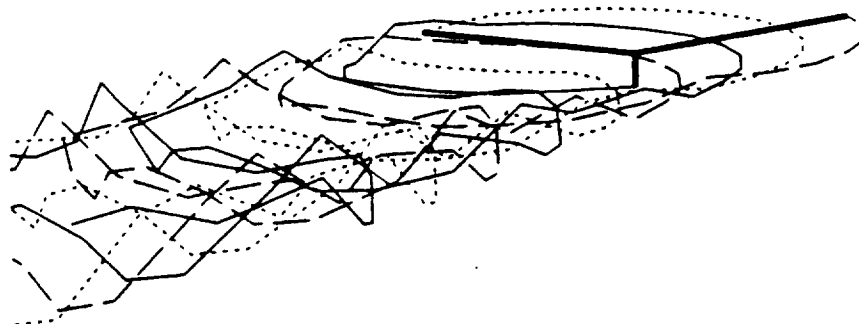
Figure 1. Calculated free wake geometry; 3 blades, $C_T/\sigma = 0.065$, $\mu = 0.14$.
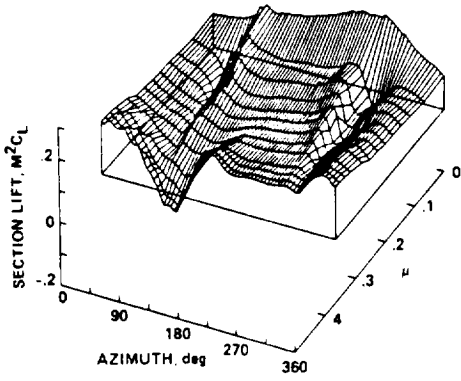
Figure 2. Rotor blade airloading in forward flight; 4 blades, solidity = 0.091, radial station = 95% R (Bousman, 1989)
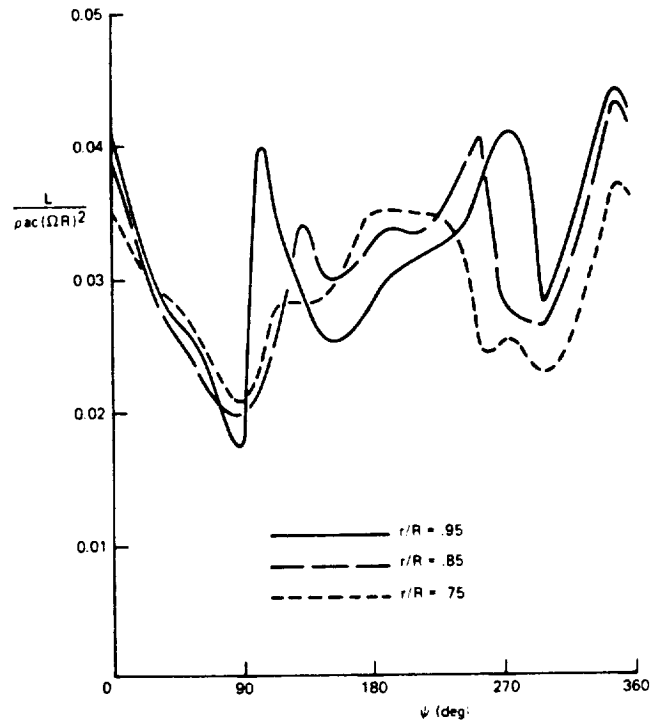
Figure 4. Measured rotor blade section lift (dimensionless), $\mu = 0.15$, $C_T/\sigma = 0.089$
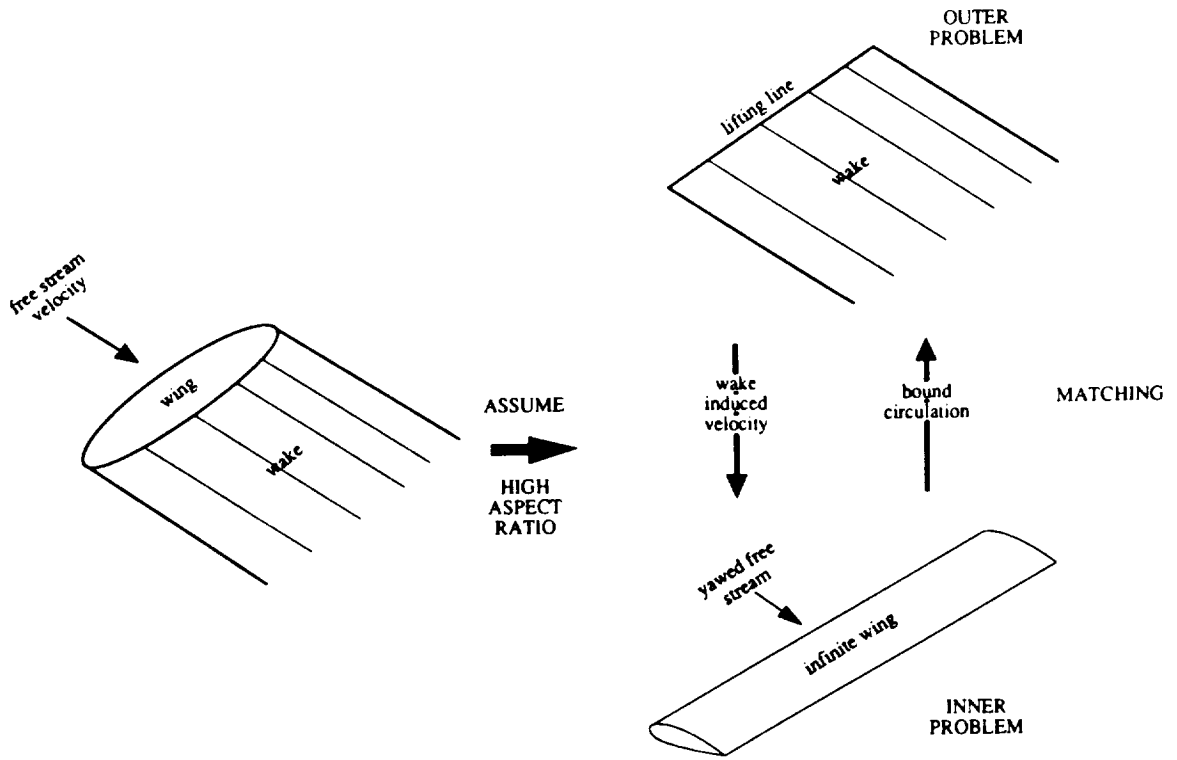
Figure 3. Lifting-line theory
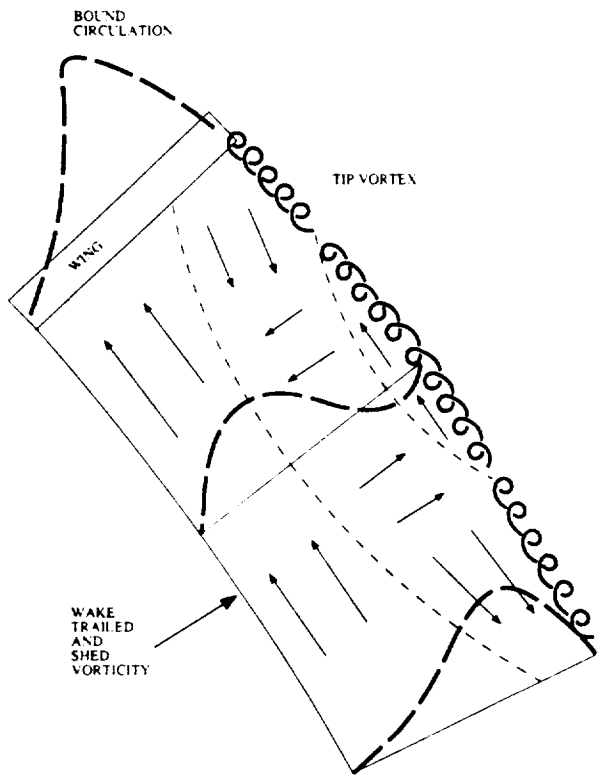
Figure 5. Rotor wake rollup
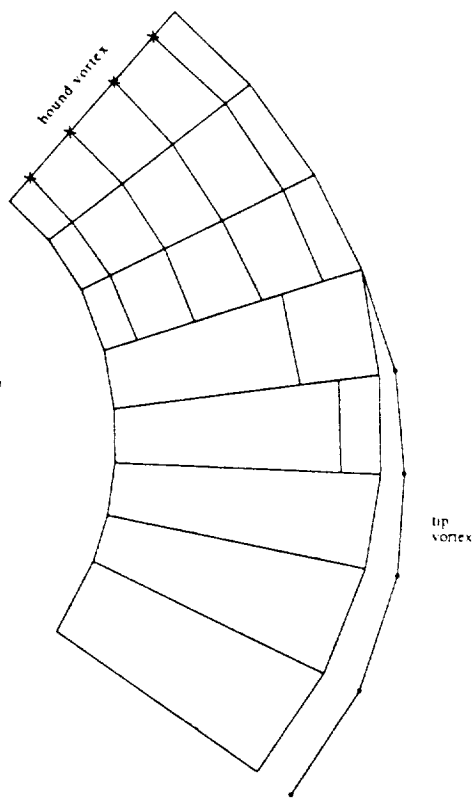
Figure 6. Rotor wake model -- sheet panels
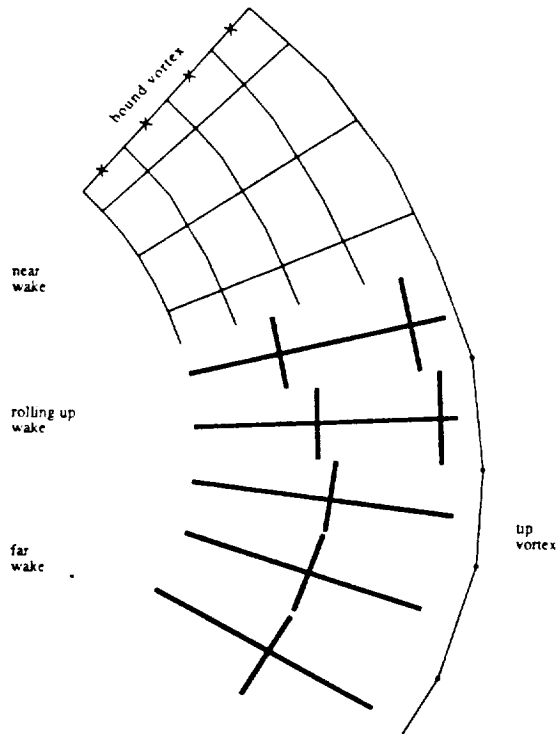
Figure 7. Rotor wake model -- line segments
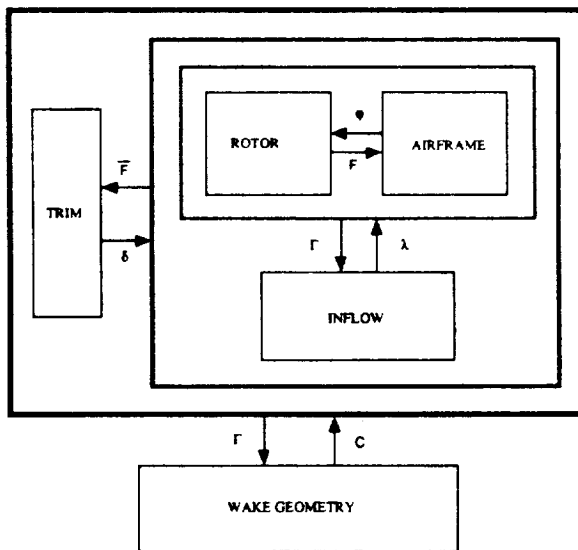
Figure 8. Partitioned solution for trim

APPENDIX

This appendix contains additional figures that accompany the lecture.

INFLUENCE OF TIP VORTEX ROLLUP POSITION ON LOADING

2 blades, solidity = .046, CT/sigma = 0.10

two-bladed rotor in hover, rectangular tip planform
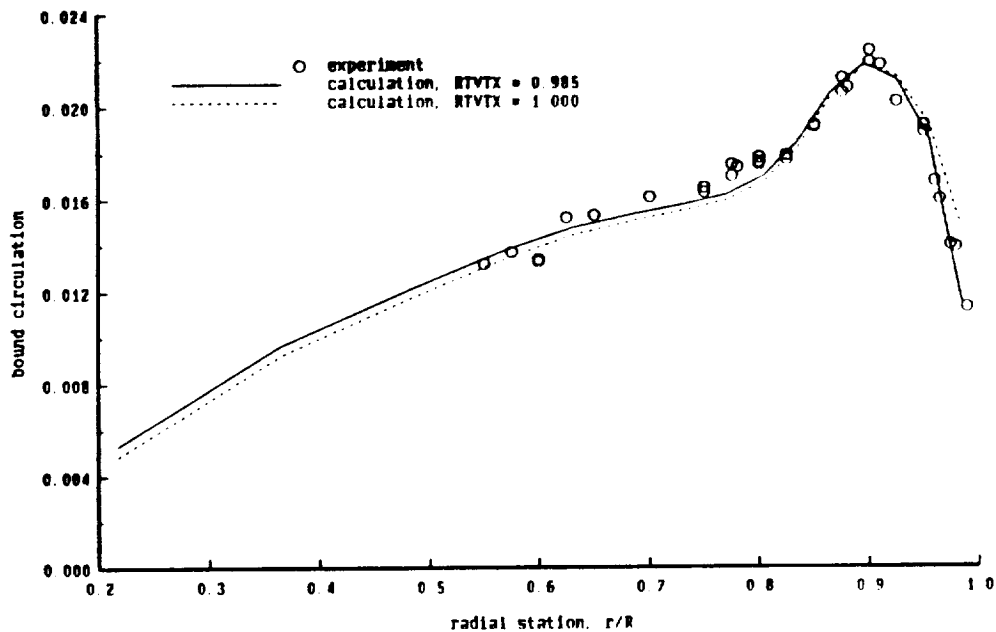
3.6.1

ROTOR BLADE SPANWISE CIRCULATION DISTRIBUTION

3 blades, solidity = 0.064, twist = -9.3 (0 for r>.91)

mu = .14, CT/sigma = .065, calculated airloads
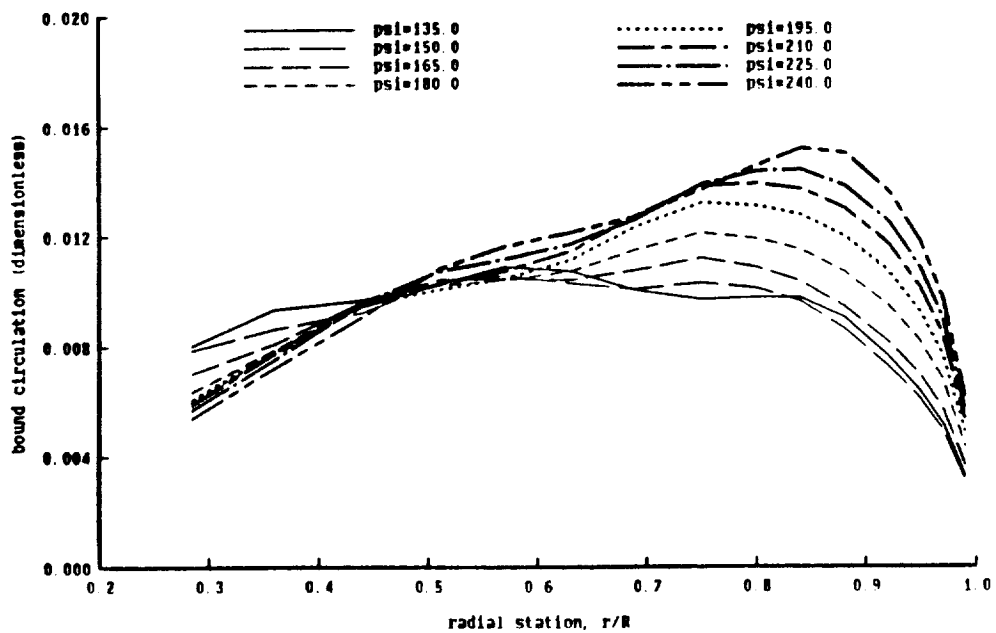
3.6.2

ROTOR BLADE SPANWISE CIRCULATION DISTRIBUTION

4 blades, solidity = 0.107 (tapered tip)
twist = -11.7 (-17.3 for r > .86 R)

mu = .36, CT/sigma = .070, alpha-shaft = -6.7, calculated airloads
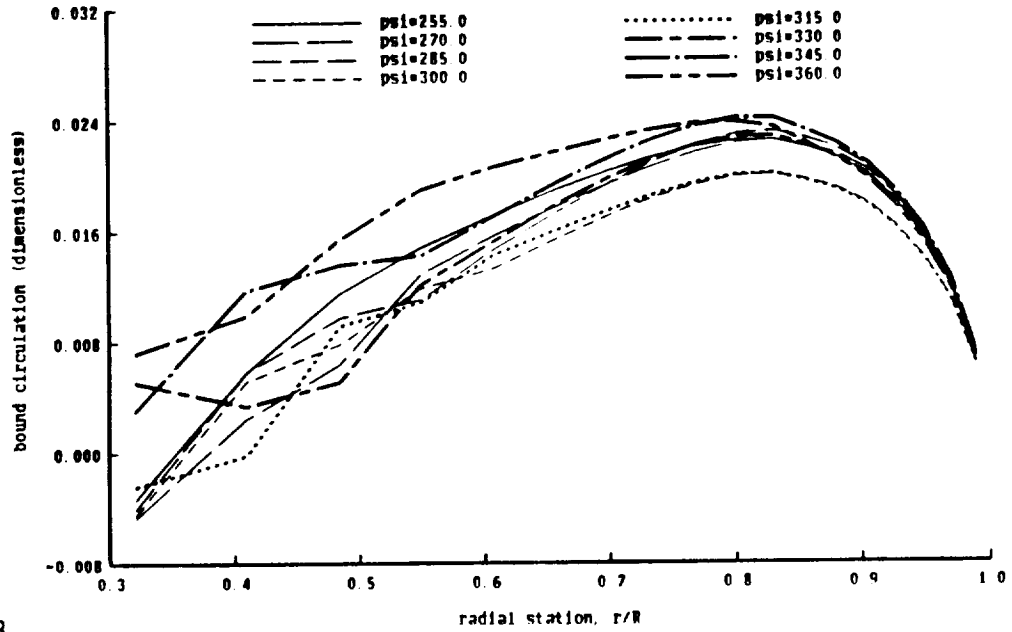
3.6.3

ROTOR BLADE SPANWISE CIRCULATION DISTRIBUTION

4 blades, solidity = 0.107 (tapered tip)
twist = -11.7 (-17.3 for r > .86 R)

mu = .36, CT/sigma = .070, alpha-shaft = -6.7, calculated airloads
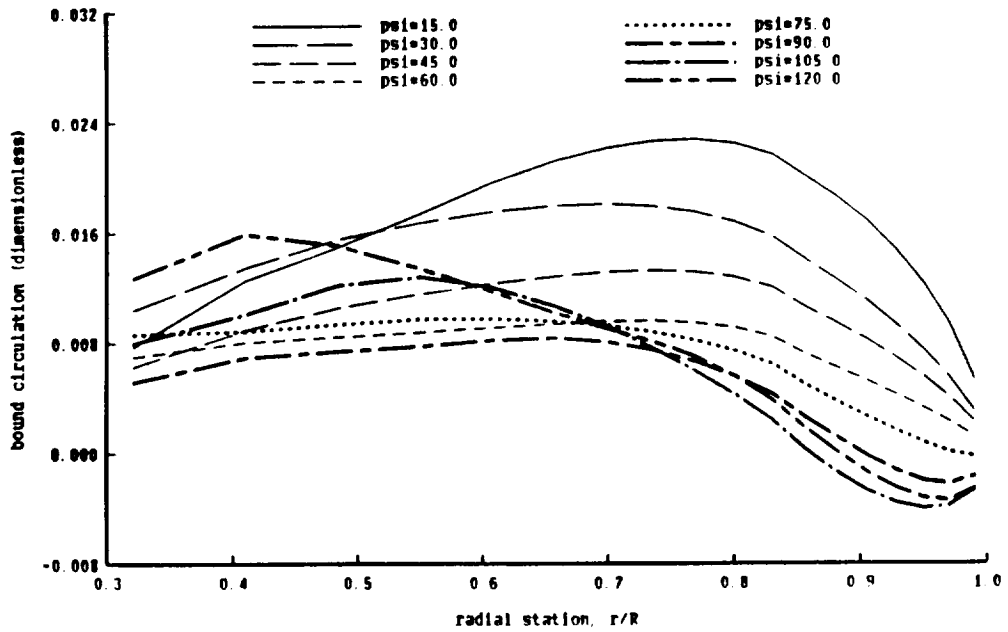
3.7.1

TIP VORTEX CORE TYPES
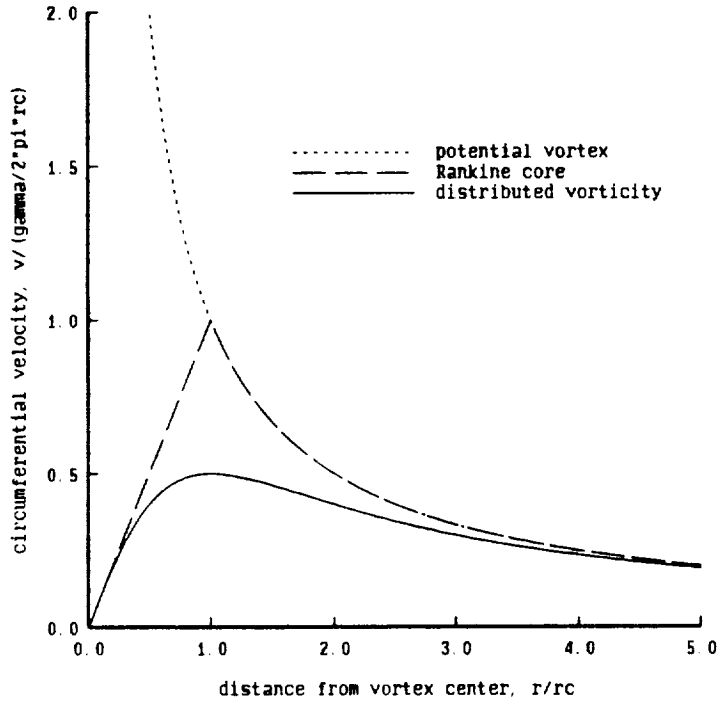
5.5.1

TIP VORTEX CORE TYPES
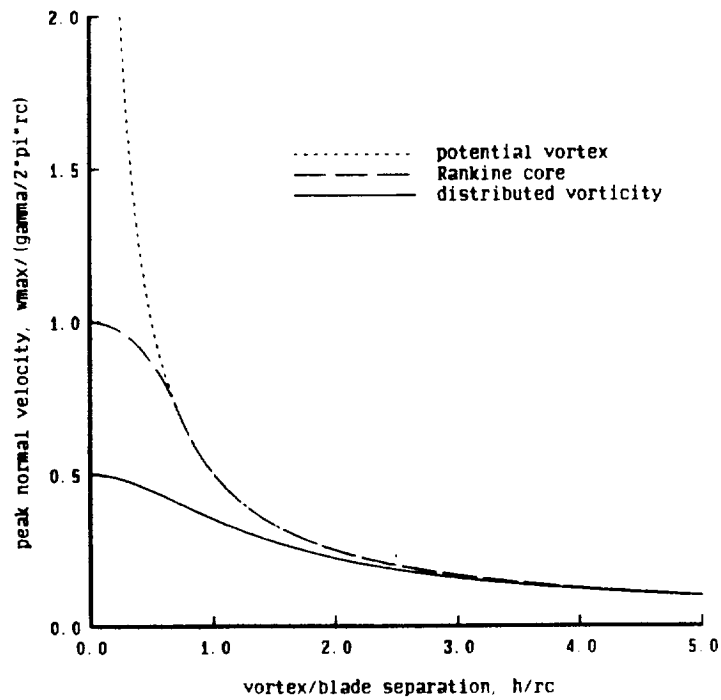
5.6.1
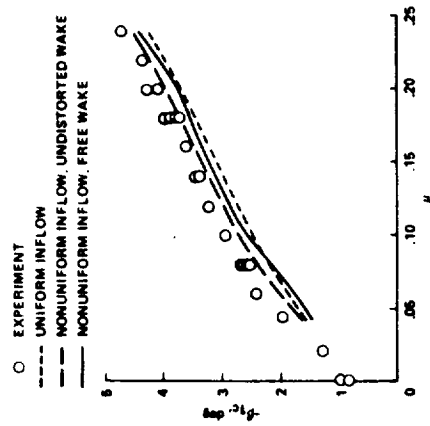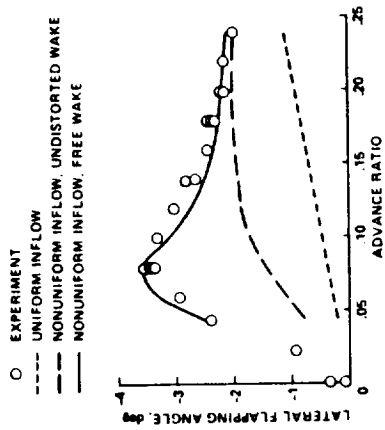
INFLUENCE OF WAKE MODEL ON LATERAL FLAPPING

4 blades, solidity = 0.089; CT/sigma = 0.08, alpha-tpp = 1 deg

O   EXPERIMENT
--- UNIFORM INFLOW
-·- NONUNIFORM INFLOW, UNDISTORTED WAKE
——— NONUNIFORM INFLOW, FREE WAKE

LATERAL FLAPPING ANGLE, deg

ADVANCE RATIO

O   EXPERIMENT
--- UNIFORM INFLOW
-·- NONUNIFORM INFLOW, UNDISTORTED WAKE
——— NONUNIFORM INFLOW, FREE WAKE

μ

6.2.2

INFLUENCE OF NONUNIFORM INFLOW AND WAKE GEOMETRY

4 blades, solidity = 0.062
CT/sigma = 0.087, mu = 0.18, r/R = 0.95

c/4 collocation point, with lifting surface correction
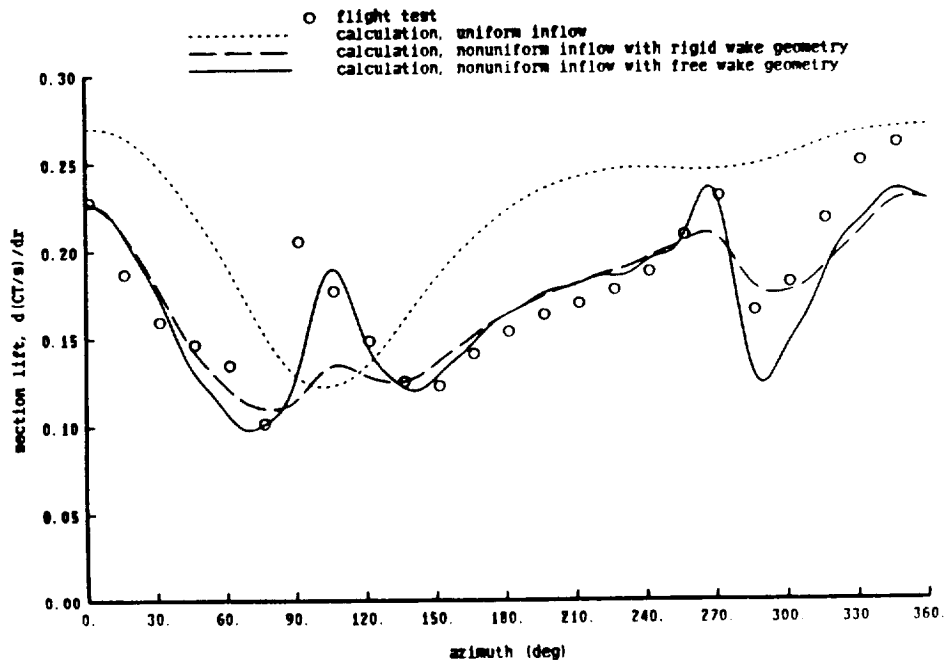
O   flight test
····· calculation, uniform inflow
— — — calculation, nonuniform inflow with rigid wake geometry
——— calculation, nonuniform inflow with free wake geometry

section lift, d(CT/s)/dr

azimuth (deg)

6.2.5

27

CL/sigma = .08, D/q = 30; free wake geometry, 3 revs wake
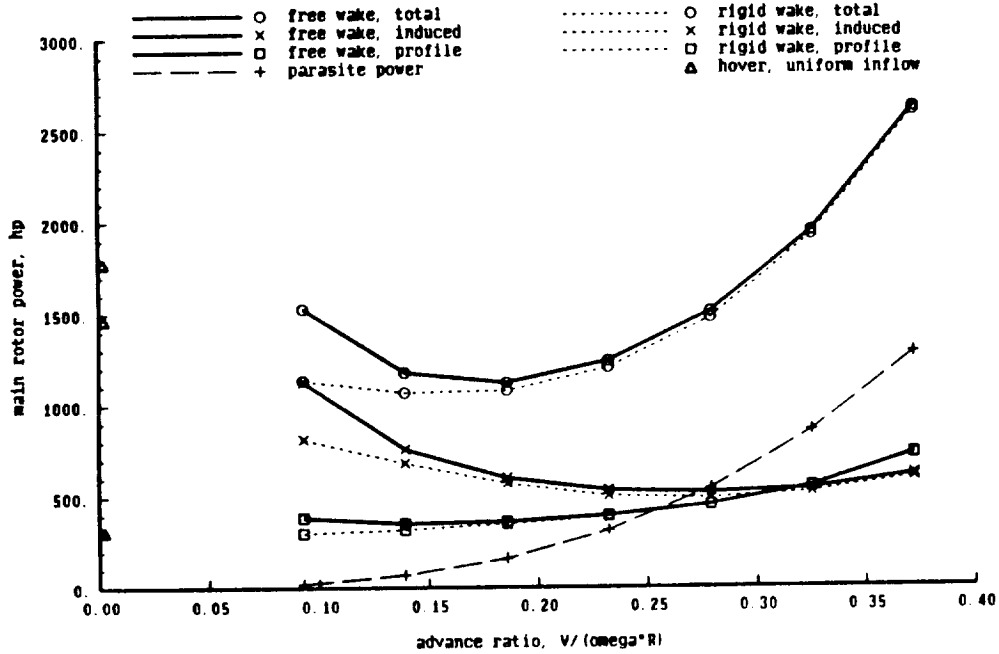
6.3.1

INFLUENCE OF NONUNIFORM INFLOW AND WAKE GEOMETRY

4 blades, solidity = 0.092 (swept tip), twist = -9

CL/sigma = .08, D/q = 30; free wake geometry, 3 revs wake

6.3.2

28
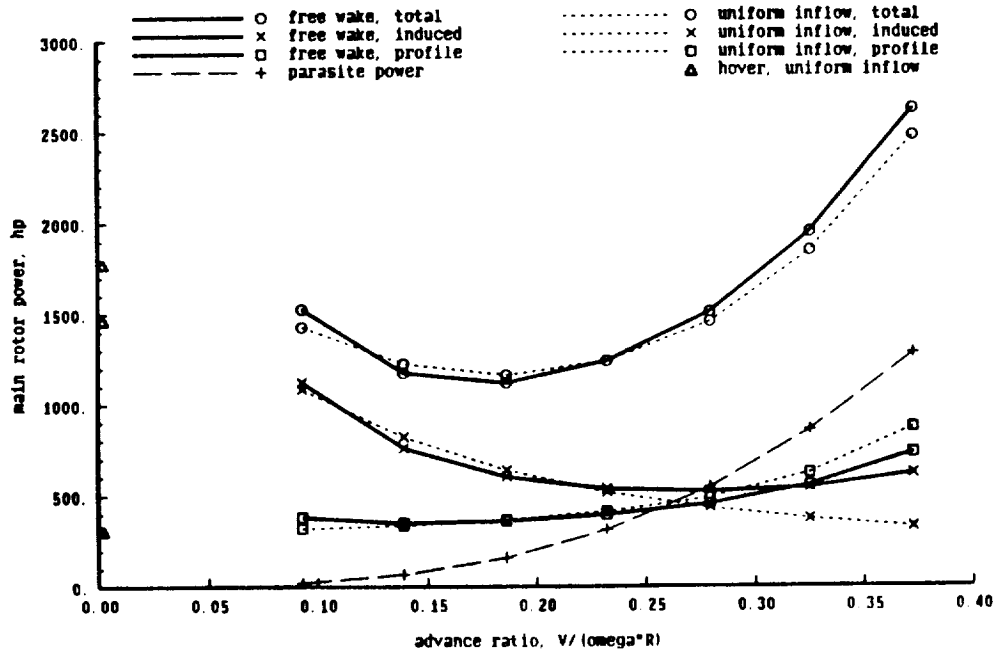
INFLUENCE OF NONUNIFORM INFLOW AND WAKE GEOMETRY

4 blades, solidity = 0.092 (swept tip), twist = -9

CL/sigma = .08, D/q = 30; free wake geometry, 3 revs wake
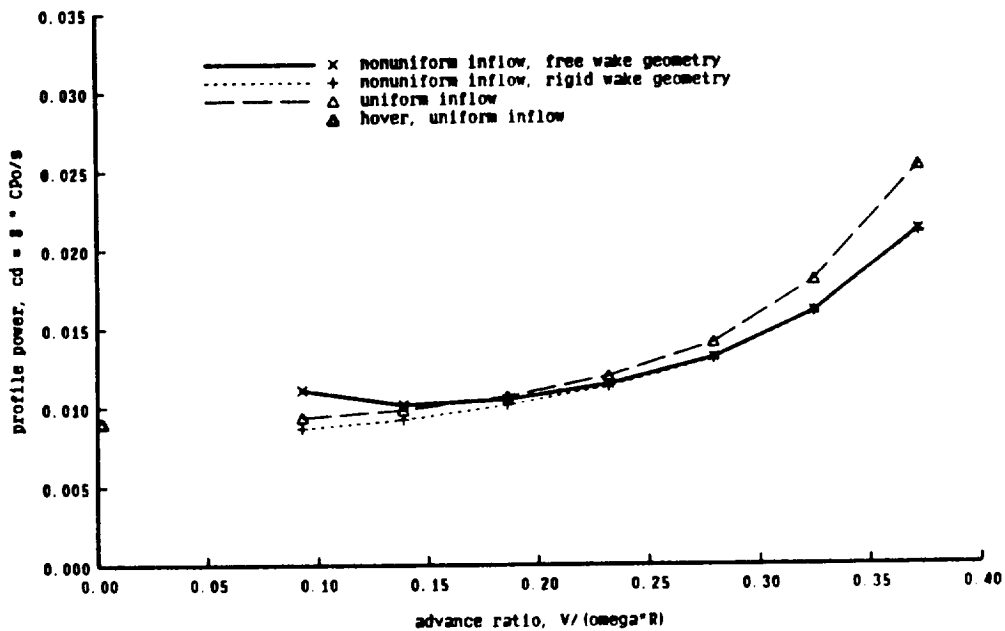
6.3.3

INFLUENCE OF NONUNIFORM INFLOW AND WAKE GEOMETRY

4 blades, solidity = 0.092 (swept tip), twist = -9

CL/sigma = .08, D/q = 30; free wake geometry, 3 revs wake
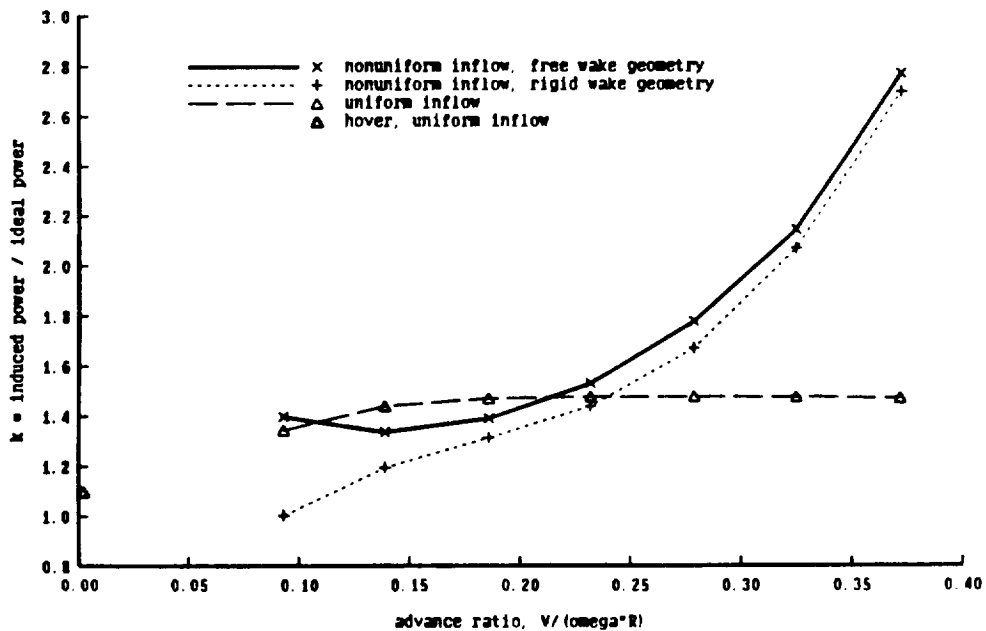
6.3.4

COMPARISON OF CALCULATED AND MEASURED LOW SPEED POWER

4 blades, solidity = 0.092 (swept tip), twist = -9

CW/s = .098; free wake geometry

————————	main rotor profile power
—·—·—·—·	+ parasite power
— — — —	+ main rotor induced power
············	+ tail rotor power
————————	+ transmission/accessory losses
□	flight test, shaft power
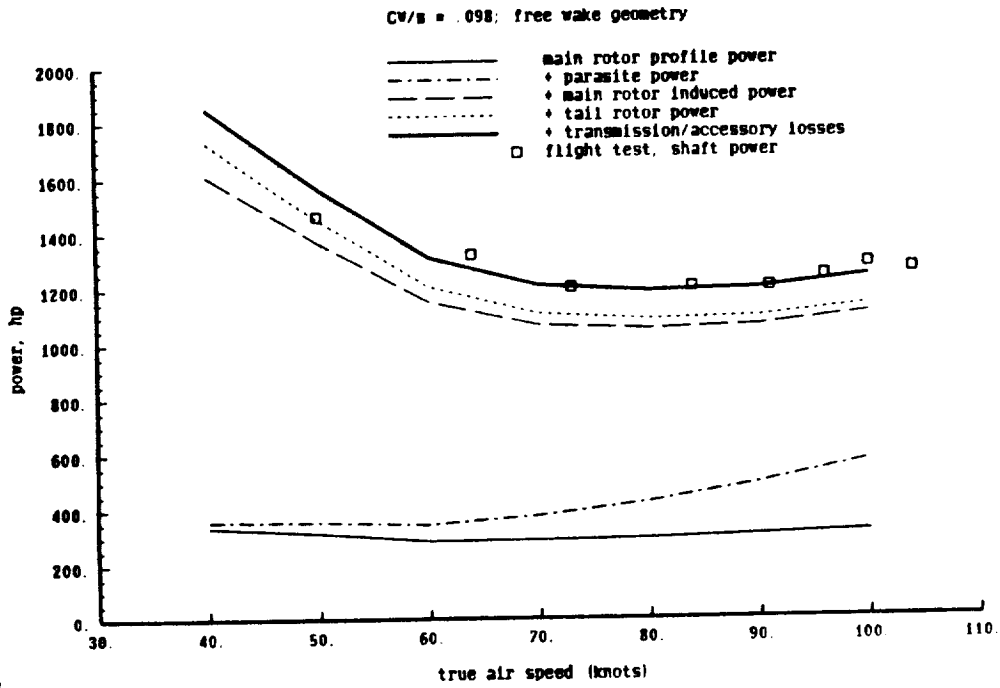
6.3.6

INFLUENCE OF CORE SIZE AND WING MODEL

model rotor, CT/sigma = 0.08, alpha-tpp = 1 deg

3c/4 coll point, no 1s correction, 2 revs wake geometry

○	experiment
————————	calculation, core = .020R = .29c
————————	calculation, core = .035R = .50c
— — — —	calculation, core = .050R = .71c
············	calculation, core = .065R = .93c

6.4.1

30

model rotor, CT/sigma = 0.08, alpha-tpp = 1 deg

c/4 coll point, no 1s correction, 2 revs wake geometry

6.4.2

model rotor, CT/sigma = 0.08, alpha-tpp = 1 deg

c/4 coll point, with 1s correction, 2 revs wake geometry
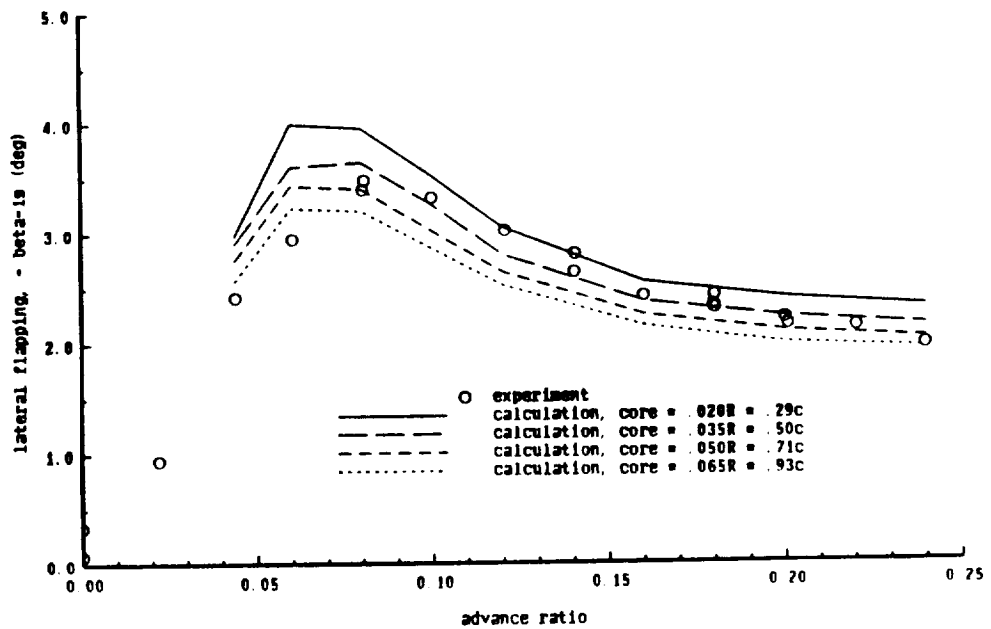
6.4.3

INFLUENCE OF CORE SIZE AND WING MODEL

3 blades, solidity = 0.064
CT/sigma = 0.065, mu = 0.14, r/R = 0.97

3c/4 collocation point,   no lifting surface correction
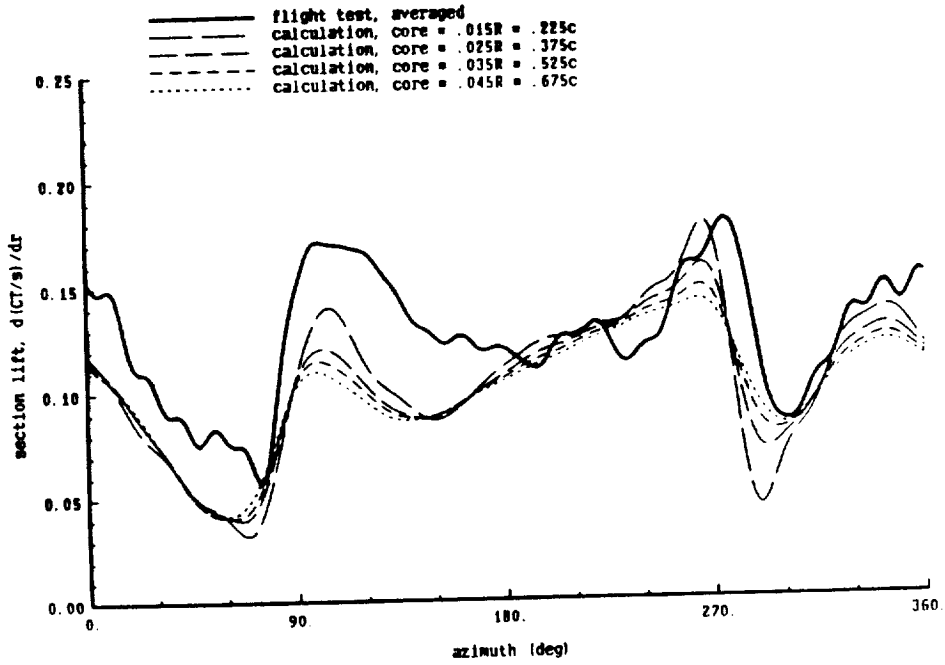
6.5.1

INFLUENCE OF CORE SIZE AND WING MODEL

3 blades, solidity = 0.064
CT/sigma = 0.065, mu = 0.14, r/R = 0.97

c/4 collocation point,   no lifting surface correction
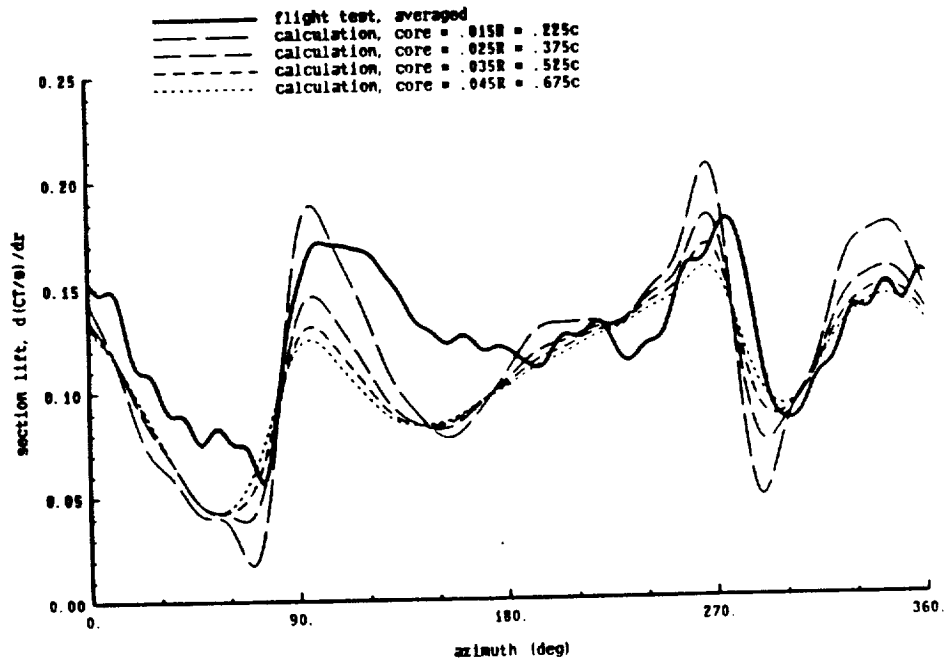
6.5.2

INFLUENCE OF CORE SIZE AND WING MODEL

3 blades, solidity = 0.064
CT/sigma = 0.065, mu = 0.14, r/R = 0.97
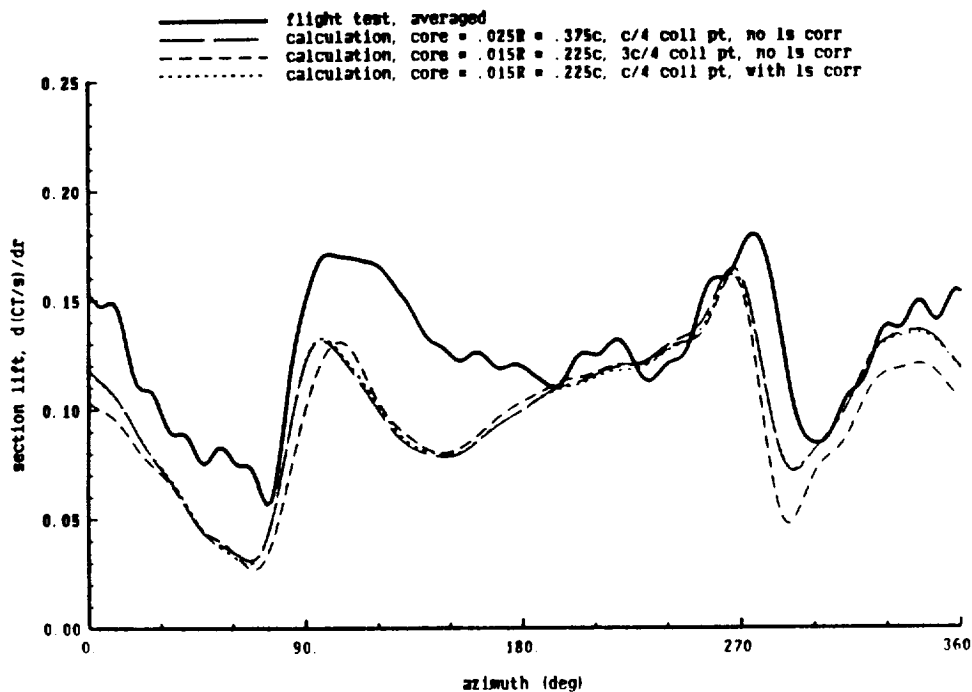
6.5.3

ROTOR BLADE SECTION AIRLOADING

4 blades, solidity = 0.092 (swept tip), twist = -9

CT/sigma = .08, mu = .09

6.5.7

33

INFLUENCE OF TIP VORTEX CORE SIZE AND WING MODEL

4 blades, solidity = 0.092 (swept tip), twist = -9

CW/s = .087; free wake geometry
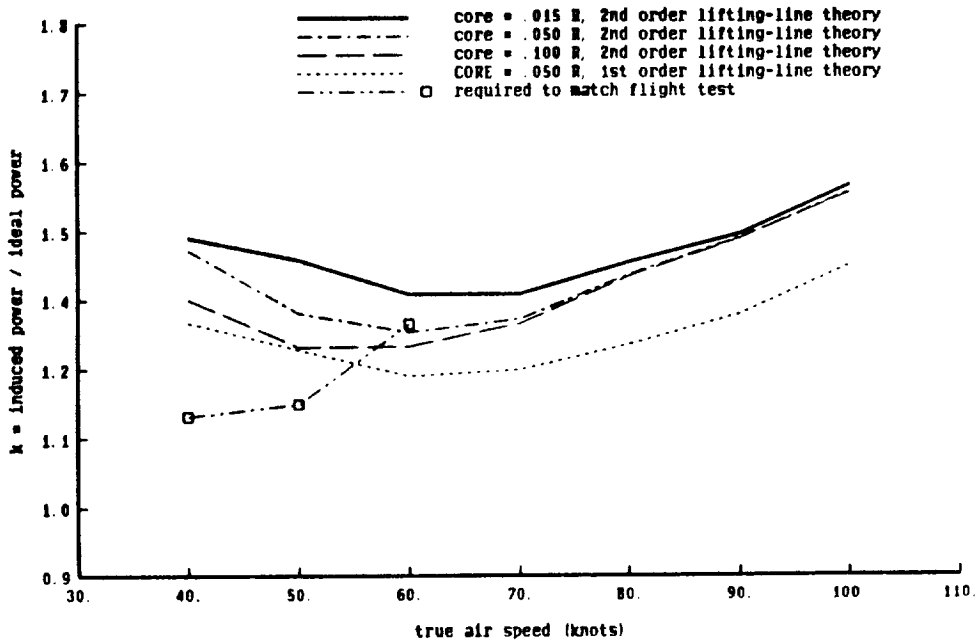
———————	core = .015 R, 2nd order lifting-line theory
—·—··—·—·	core = .050 R, 2nd order lifting-line theory
—— — ——	core = .100 R, 2nd order lifting-line theory
·············	CORE = .050 R, 1st order lifting-line theory
—··—··—· □	required to match flight test

6.6.1

INFLUENCE OF WING MODEL

4 blades, solidity = 0.092 (swept tip), twist = -9

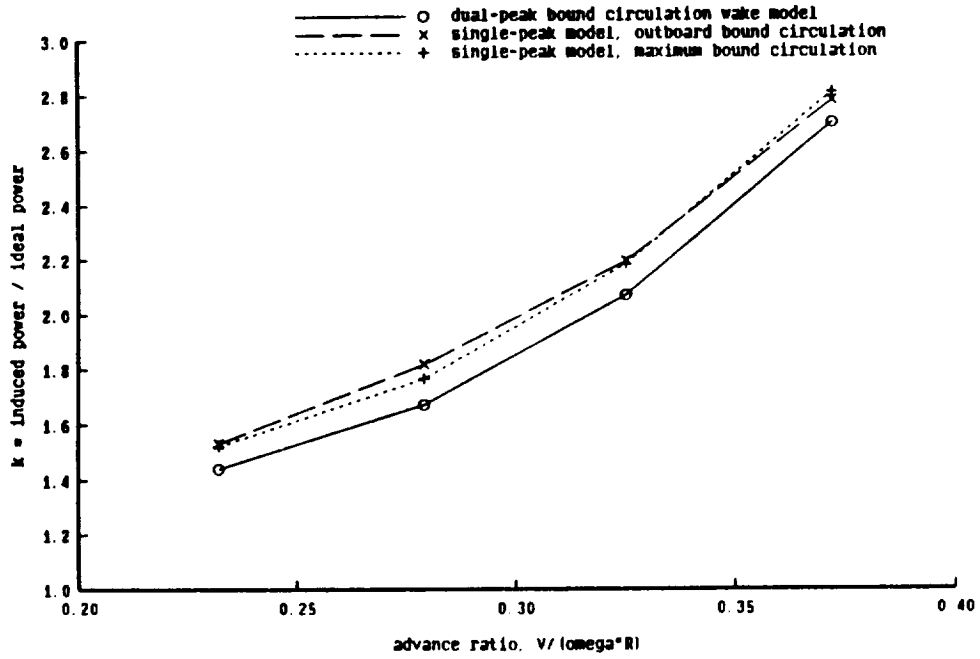CL/sigma = .08, D/q = 30; free wake geometry, 3 revs wake

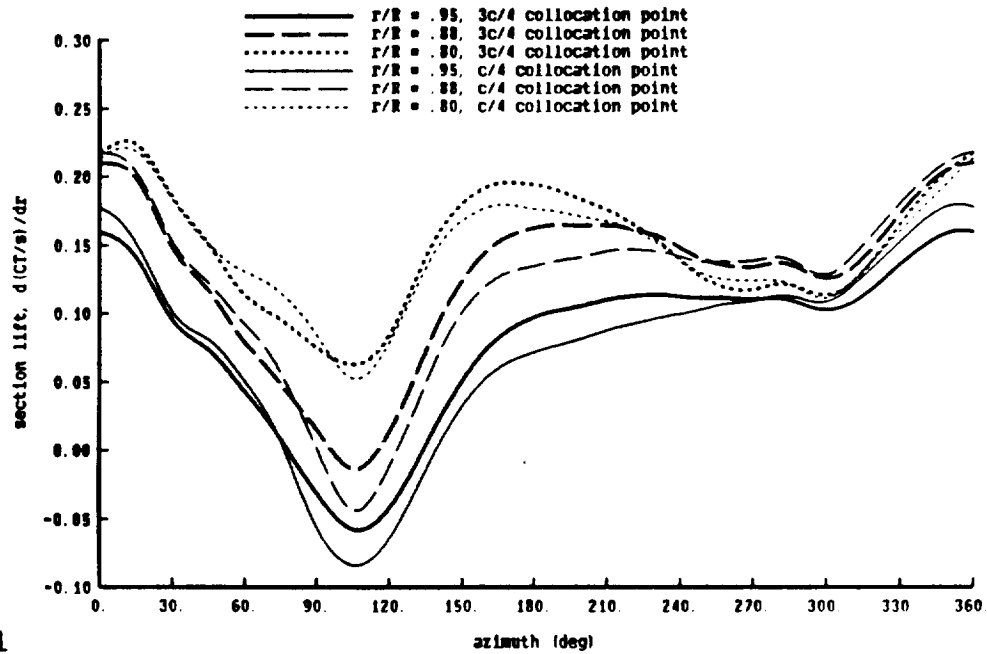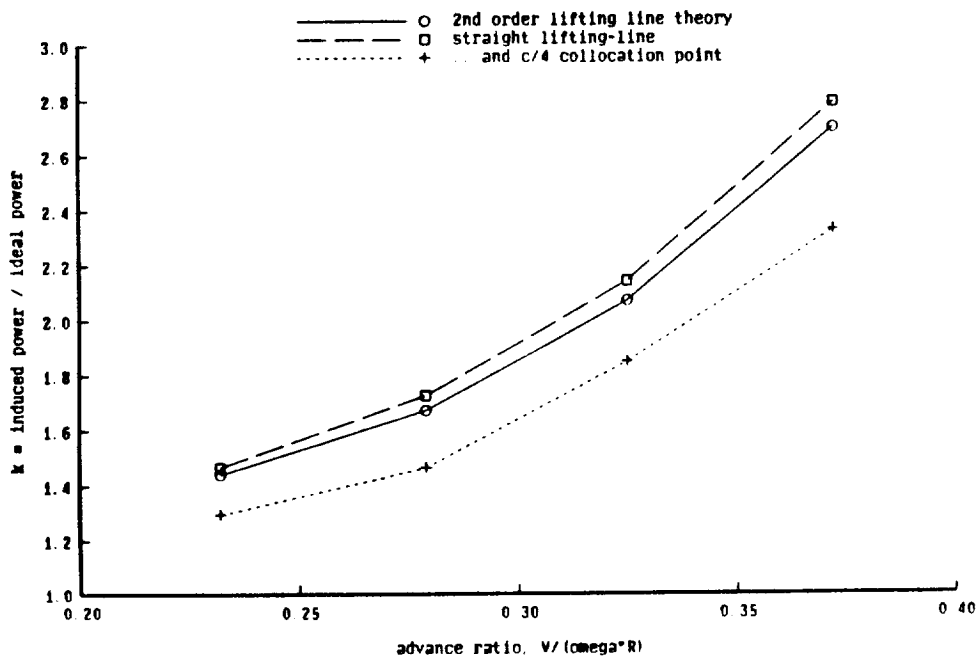|	
——————— O	2nd order lifting line theory, core = .015 R
—— —— — □	straight lifting-line
············· +	.. and c/4 collocation point
—··—··—· x	.. and core = .050 R

6.6.2

34

INFLUENCE OF TIP VORTEX CORE SIZE AND WING MODEL

4 blades, solidity = 0.092 (swept tip), twist = -9

CV/s = .109; free wake geometry

——————	core = .015 R, 2nd order lifting-line theory
—·—·—·	core = .050 R, 2nd order lifting-line theory
— — —	core = .100 R, 2nd order lifting-line theory
·········	core = .050 R, 1st order lifting-line theory

6.6.3

INFLUENCE OF INBOARD BLADE-VORTEX INTERACTION

4 blades, solidity = 0.062
CT/sigma = 0.087, mu = 0.18, r/R = 0.95

c/4 coll point, with 1s correction, free wake geometry

O	flight test
——————	calculation, core radius for inboard stations = .10
·········	calculation, core radius for inboard stations = .01

6.7.4

35
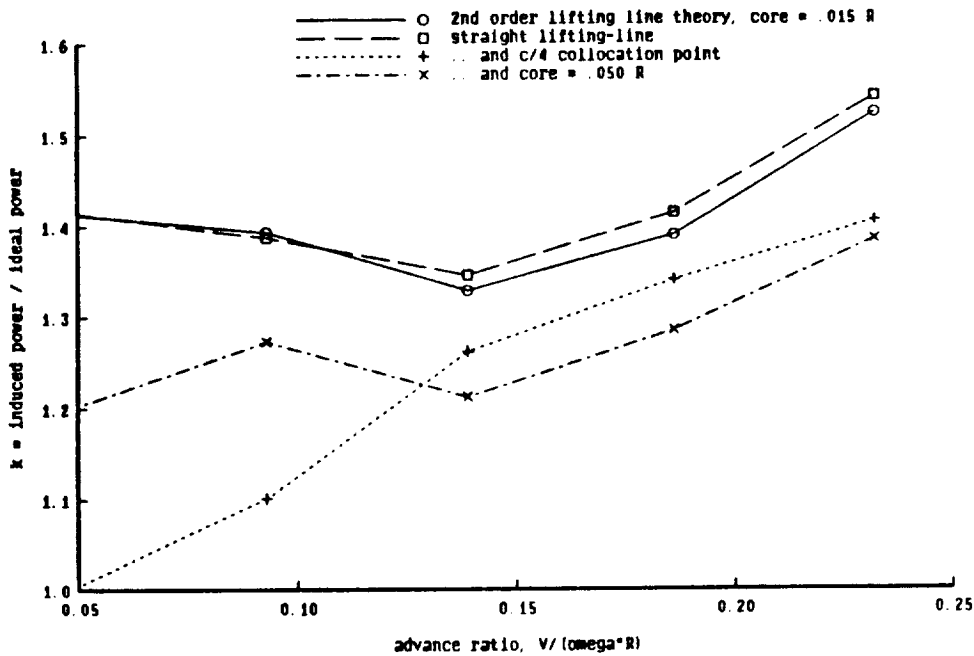
INFLUENCE OF INBOARD BLADE-VORTEX INTERACTION

4 blades, solidity = 0.062
CT/sigma = 0.087, mu = 0.18, r/R = 0.75

c/4 coll point, with 1s correction, free wake geometry
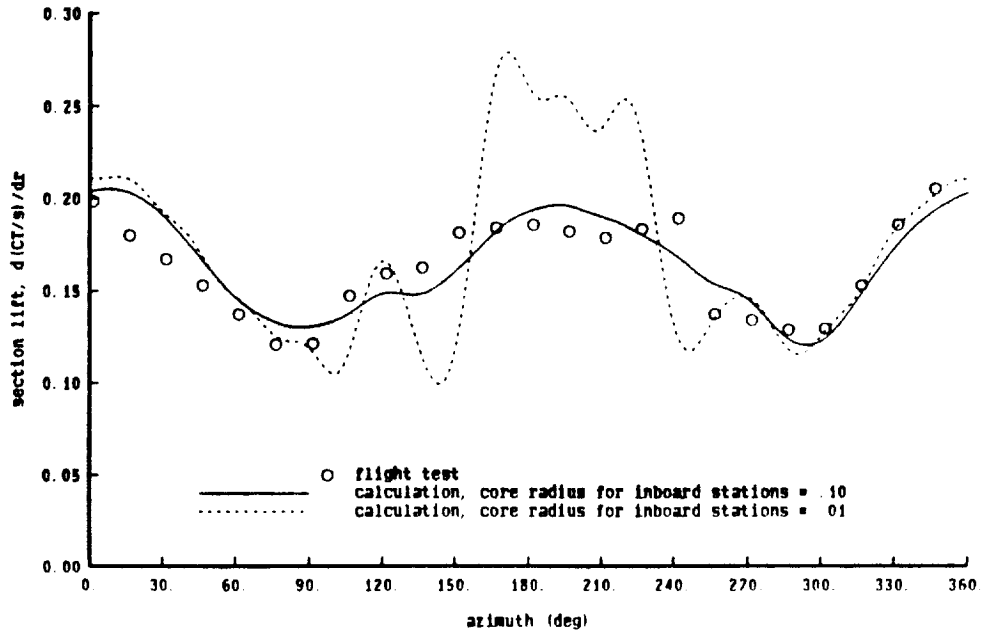
6.7.5

CALCULATED FREE WAKE GEOMETRY
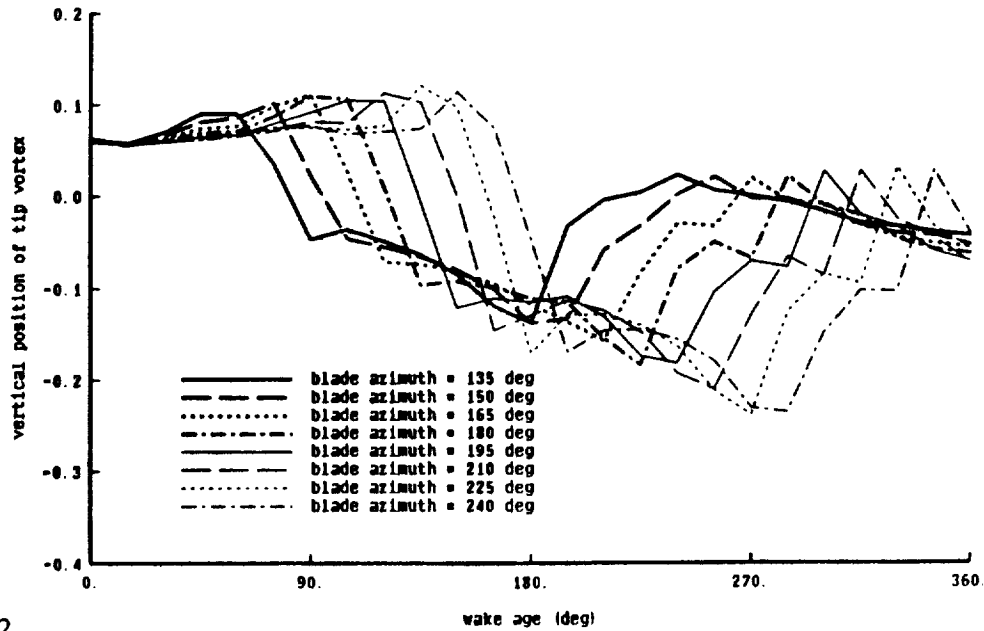
4 blades, solidity = 0.092; CT/sigma = 0.08, mu = 0.09

6.9.2

36

CALCULATED FREE WAKE GEOMETRY

4 blades, solidity = 0.092; CT/sigma = 0.08, mu = 0.09

blade azimuth = 255 deg
blade azimuth = 270 deg
blade azimuth = 285 deg
blade azimuth = 300 deg
blade azimuth = 315 deg
blade azimuth = 330 deg
blade azimuth = 345 deg
blade azimuth = 360 deg
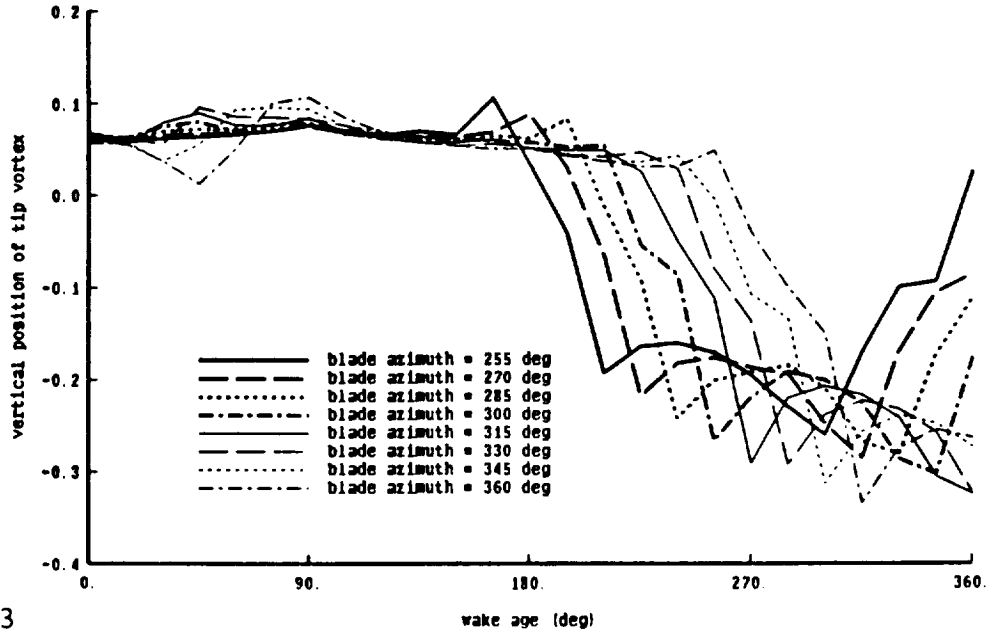
6.9.3

INFLUENCE OF NONUNIFORM INFLOW

4 blades, solidity = 0.062
CT/sigma = 0.091, mu = 0.29, r/R = 0.95

c/4 collocation point, with lifting surface correction

O   flight test
....   calculation, uniform inflow
————   calculation, nonuniform inflow
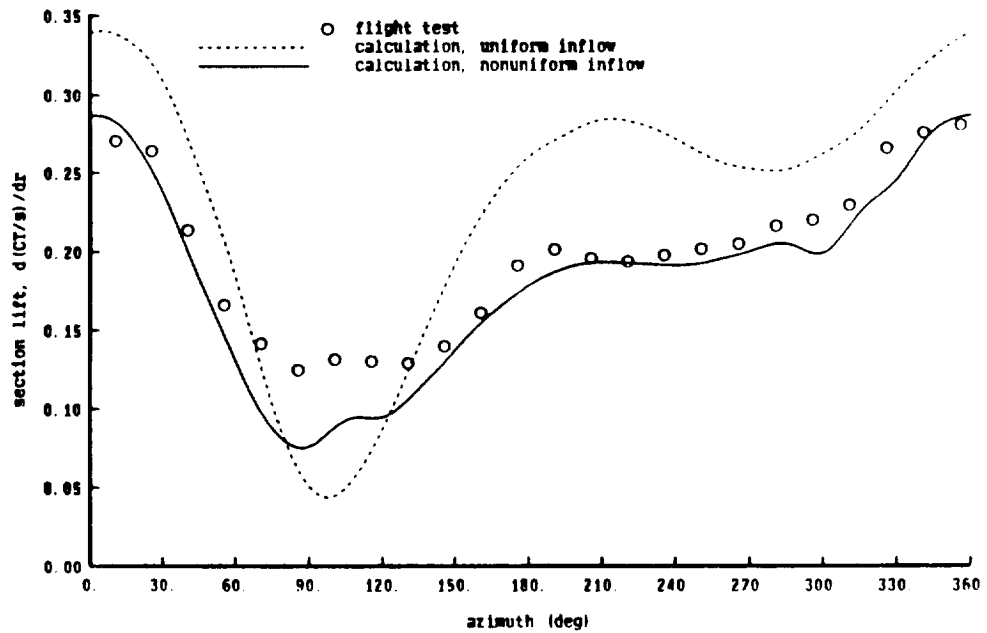
7.1.1

INFLUENCE OF NONUNIFORM INFLOW

4 blades, solidity = 0.082 (swept tip)
CT/sigma = 0.075, 160 knots, X/q = 24, r/R = 0.95
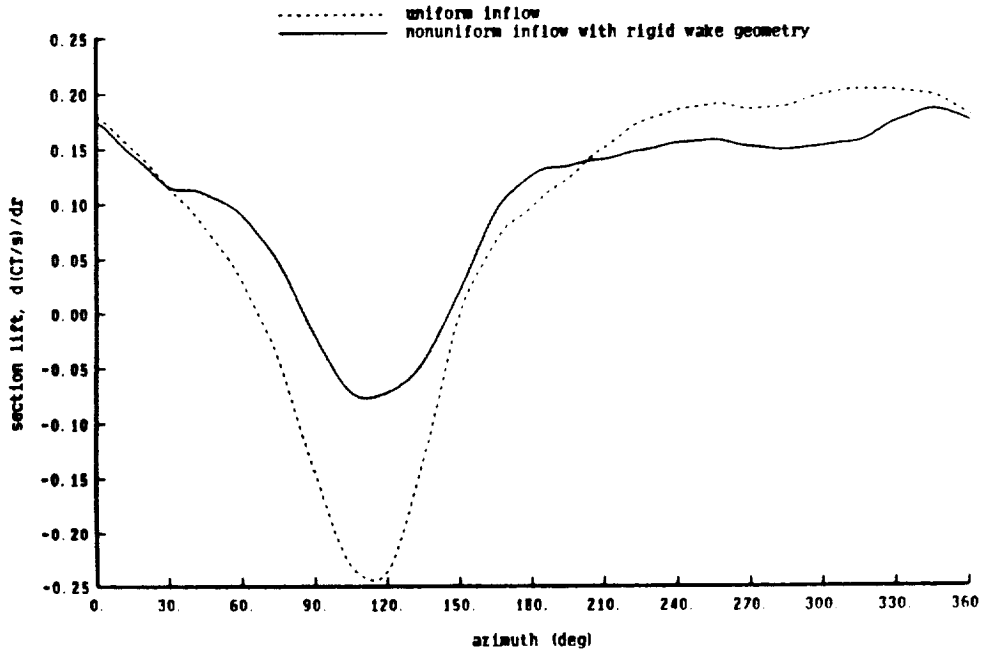
7.1.4

INFLUENCE OF DUAL-PEAK WAKE MODEL

4 blades, solidity = 0.107 (tapered tip)

Run 222, mu = .36, CT/sigma = .070, alpha-shaft = -6.7, r/R = .95

7.2.1

38
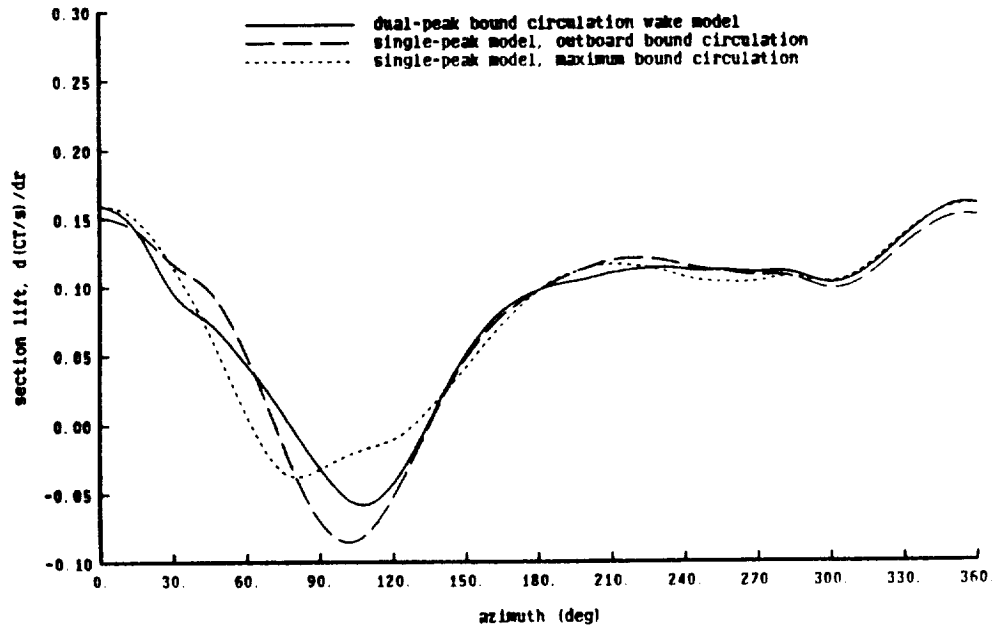
INFLUENCE OF DUAL-PEAK WAKE MODEL

4 blades, solidity = 0.062

mu = .39, CT/sigma = .059, alpha-shaft = 0, r/R = .95
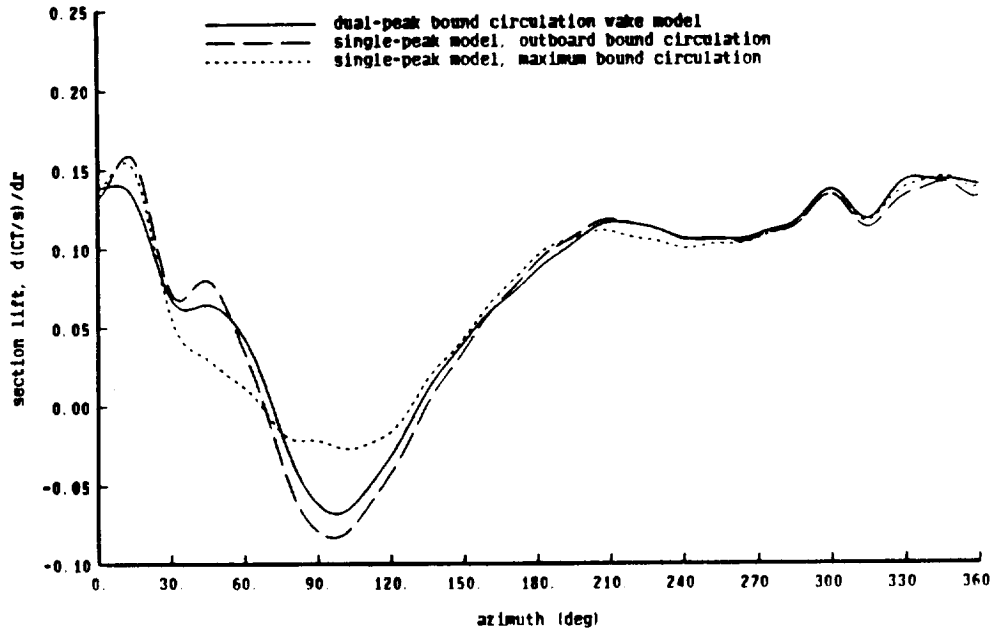
7.2.5

COMPARISON OF CALCULATED AND MEASURED SECTION LIFT

4 blades, solidity = 0.091 (swept tip)
CT/sigma = 0.08, mu = 0.38, r/R = 0.92
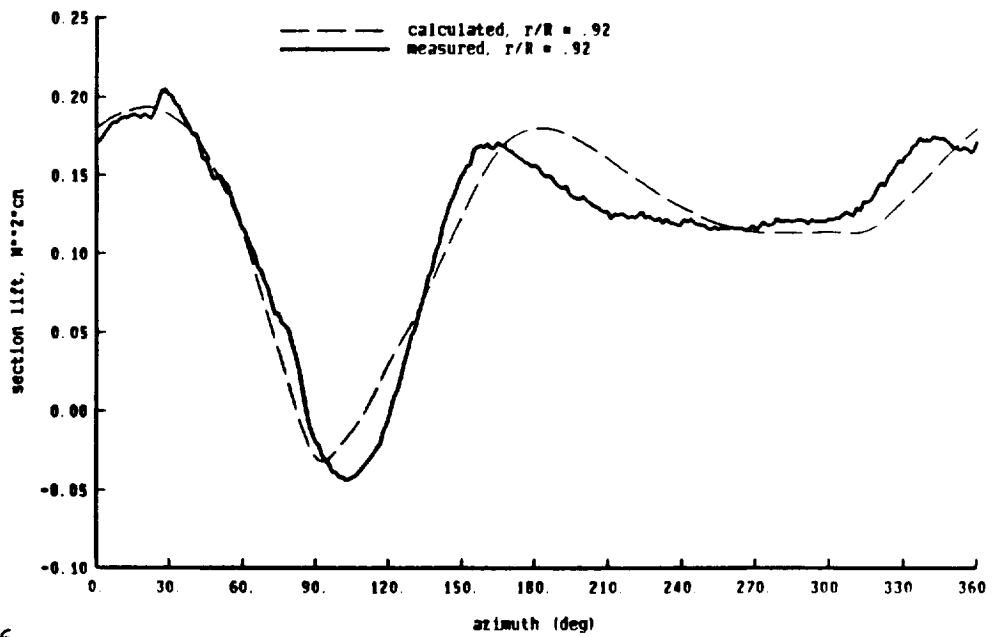
7.2.6

DUAL-PEAK WAKE MODEL

4 blades, solidity = .107; mu = 0.30, CT/sigma = 0.07
Dadone, et al. (1989)
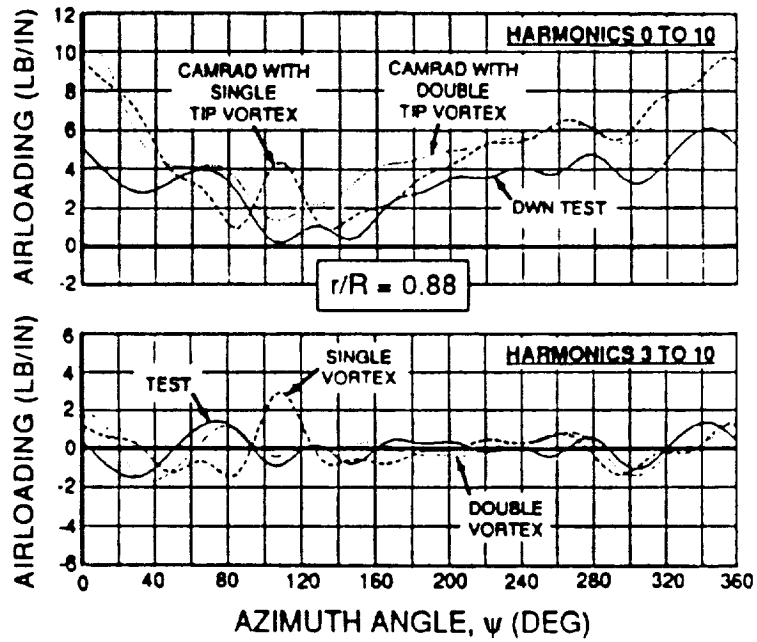
7.2.7

DUAL-PEAK WAKE MODEL: INFLUENCE OF INBOARD ROLLUP

4 blades, solidity = 0.062

mu = .39, CT/sigma = .059, alpha-shaft = 0, r/R = .95, dual-peak model
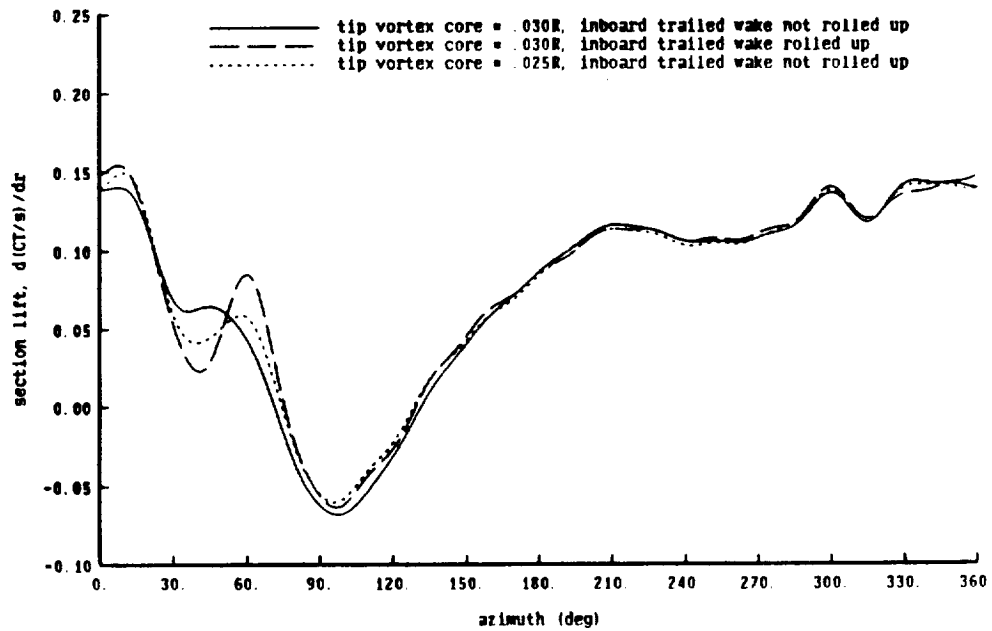
7.2.8

INFLUENCE OF DUAL-PEAK WAKE MODEL

4 blades, solidity = 0.092 (swept tip), twist = -9

CL/sigma = .08, D/q = 30; rigid wake geometry, 3 revs wake

7.3.2

INFLUENCE OF WING MODEL

4 blades, solidity = 0.107 (tapered tip)

Run 222, mu = .36, CT/sigma = .070, alpha-shaft = -6.7, dual-peak wake model

7.4.1

41

INFLUENCE OF WING MODEL

4 blades, solidity = 0.092 (swept tip), twist = -9

CL/sigma = .08, D/q = 30; rigid wake geometry, 3 revs wake

```
———————— O   2nd order lifting line theory
— — — — □   straight lifting-line
·············· +   .. and c/4 collocation point
```


7.4.5

y-axis: k = induced power / ideal power
x-axis: advance ratio, V/(omega*R)

INFLUENCE OF WING AERODYNAMIC CORRECTIONS

4 blades, solidity = 0.092 (swept tip), twist = -9

CL/sigma = .08, D/q = 30; rigid wake geometry, 3 revs wake

```
———————— O   radial drag, yawed flow and sweep corrections
—·—·—·— x   no radial drag
·············· □   without yawed flow corrections
— — — — +   without sweep corrections
```


7.4.10

y-axis: profile power, cd = 8 * Cpo/s
x-axis: advance ratio, V/(omega*R)
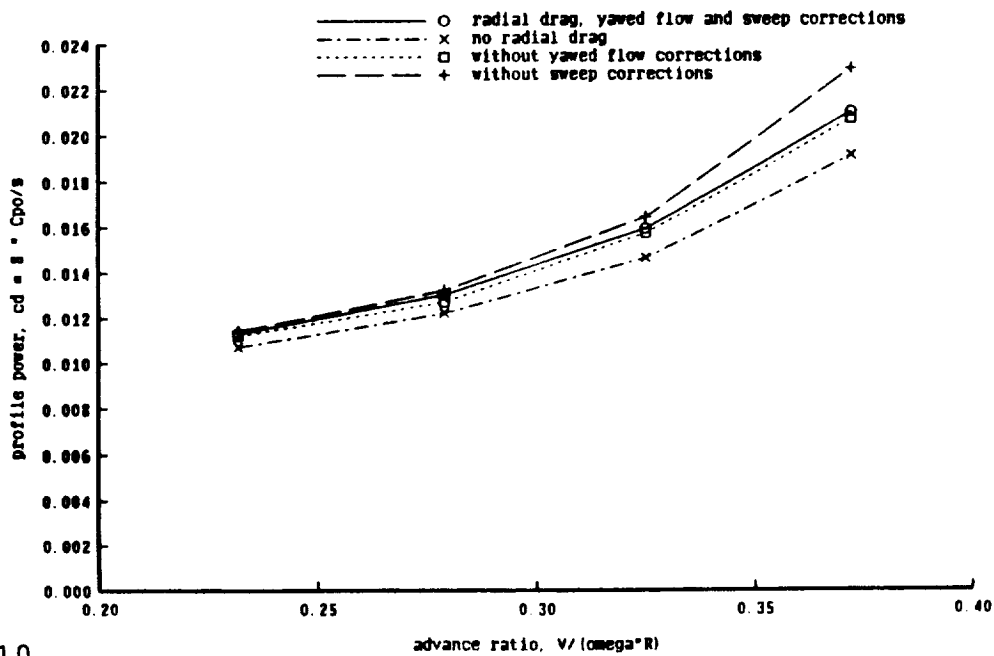
COMPARISON OF CALCULATED AND MEASURED SECTION LIFT

4 blades, solidity = 0.091 (swept tip)
CT/sigma = 0.08, mu = 0.38, r/R = 0.95
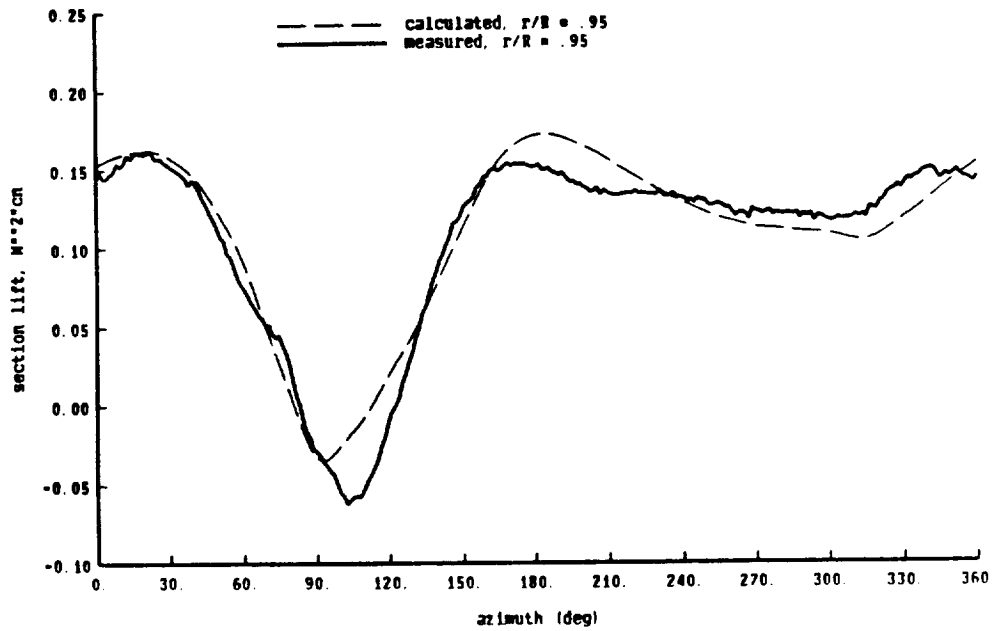
7.6.3

INFLUENCE OF WING MODEL AND AERODYNAMIC CORRECTIONS

4 blades, solidity = 0.091 (swept tip)
CT/sigma = 0.08, mu = 0.38, r/R = 0.95

elastic blade

7.6.5

43
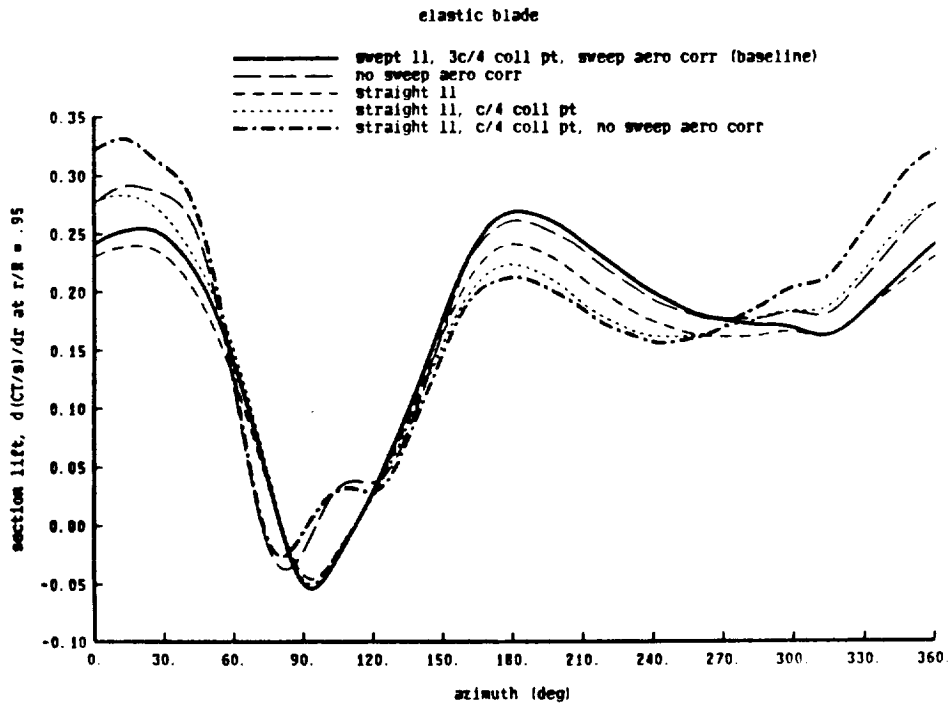
COMPARISON OF CALCULATED AND MEASURED SECTION MOMENT

4 blades, solidity = 0.091 (swept tip)
CT/sigma = 0.08, mu = 0.38, r/R = 0.92
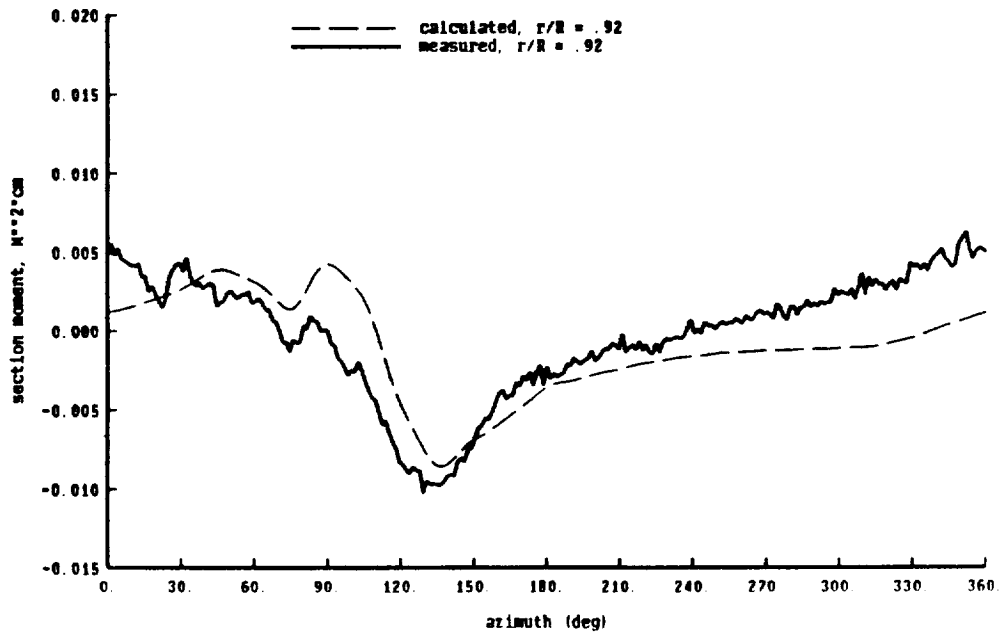
7.7.1

COMPARISON OF CALCULATED AND MEASURED SECTION MOMENT

4 blades, solidity = 0.091 (swept tip)
CT/sigma = 0.08, mu = 0.38, r/R = 0.95

7.7.2

44
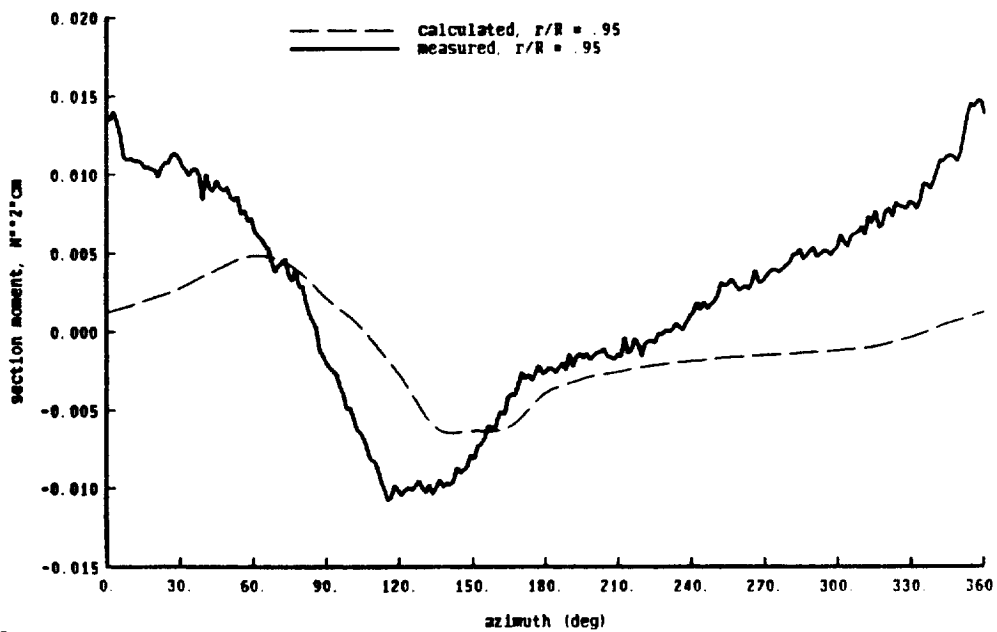
ROTOR BLADE SPANWISE CIRCULATION DISTRIBUTION

3 blades, solidity = 0.064, twist = -9.3 (0 for r>.91)

mu = .14, CT/sigma = .065, calculated airloads
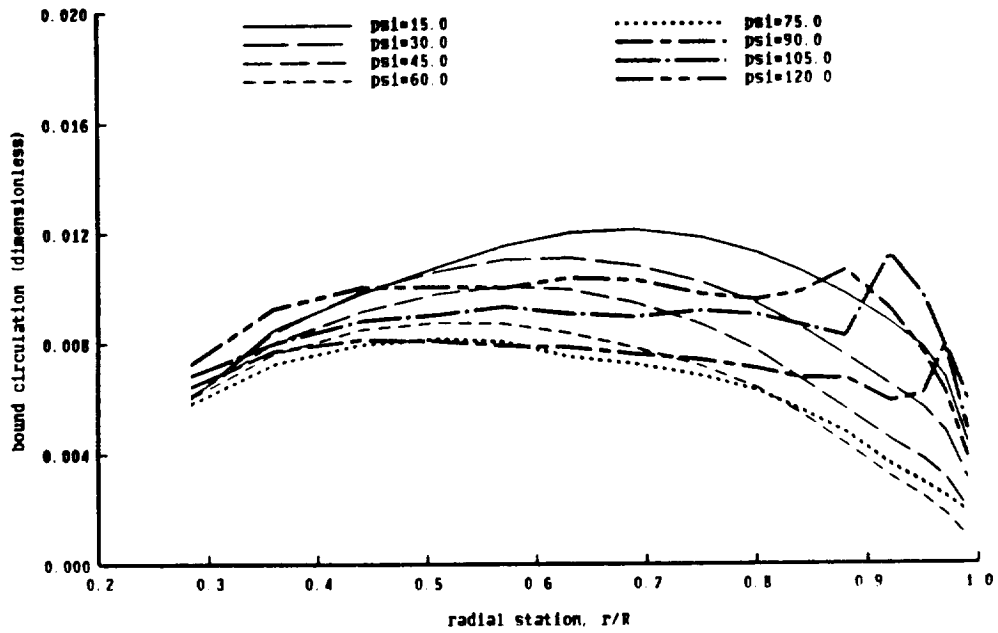
7.8.1

ROTOR BLADE SPANWISE CIRCULATION DISTRIBUTION

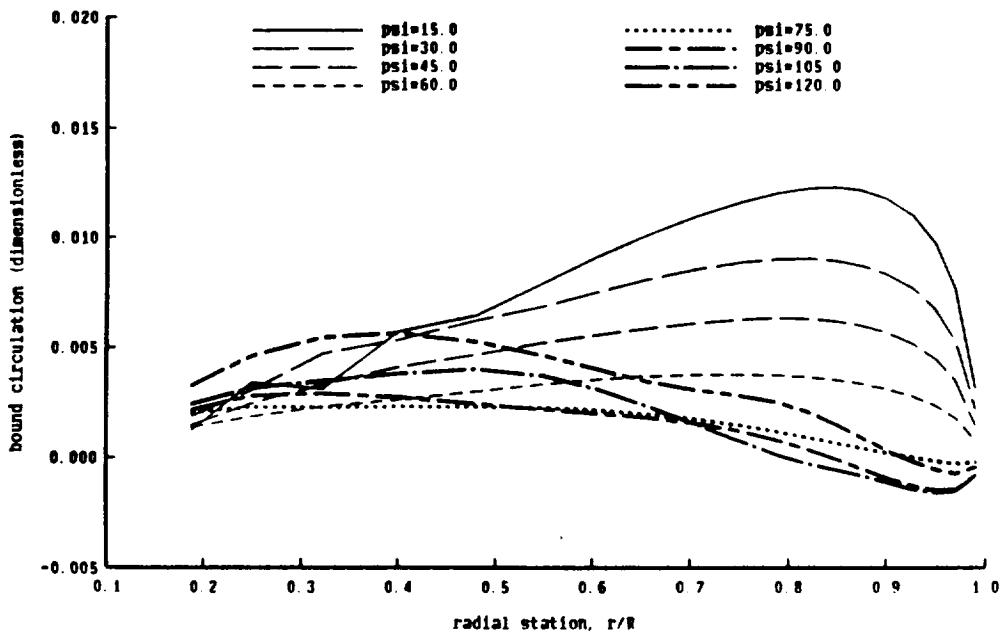4 blades, solidity = 0.092 (swept tip), twist = -9

CT/sigma = .08, mu = .09

7.8.6

45
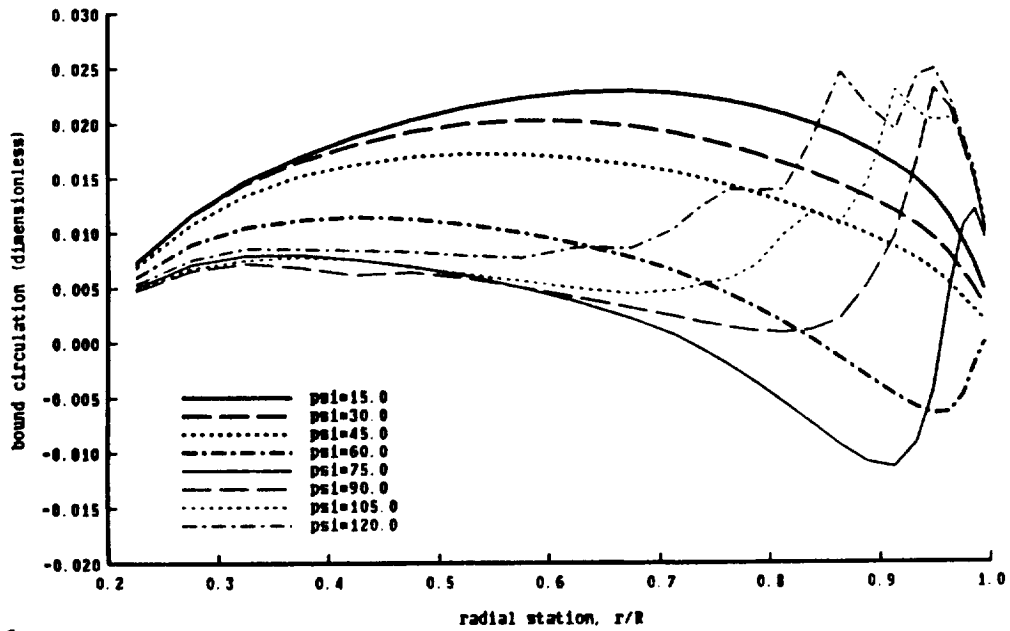
ROTOR BLADE SPANWISE CIRCULATION DISTRIBUTION

4 blades, solidity = 0.092 (swept tip), twist = -9

CT/sigma = .08, mu = .09
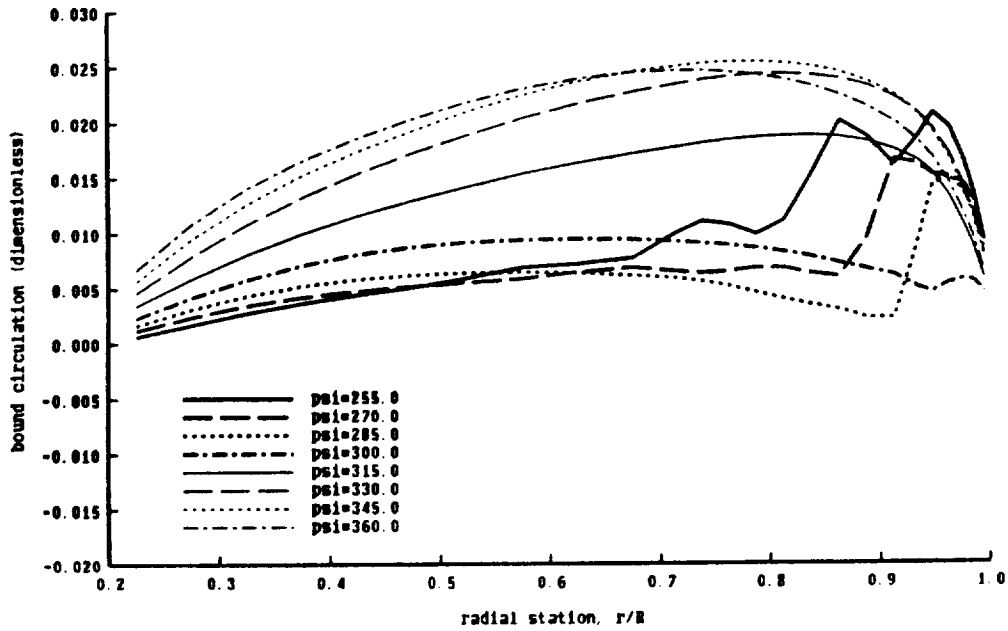
7.8.8

ROTOR BLADE SPANWISE CIRCULATION DISTRIBUTION

4 blades, solidity = 0.082 (swept tip), nonlinear twist

V = 60 knots, CT/sigma = 0.075, X/q = 24
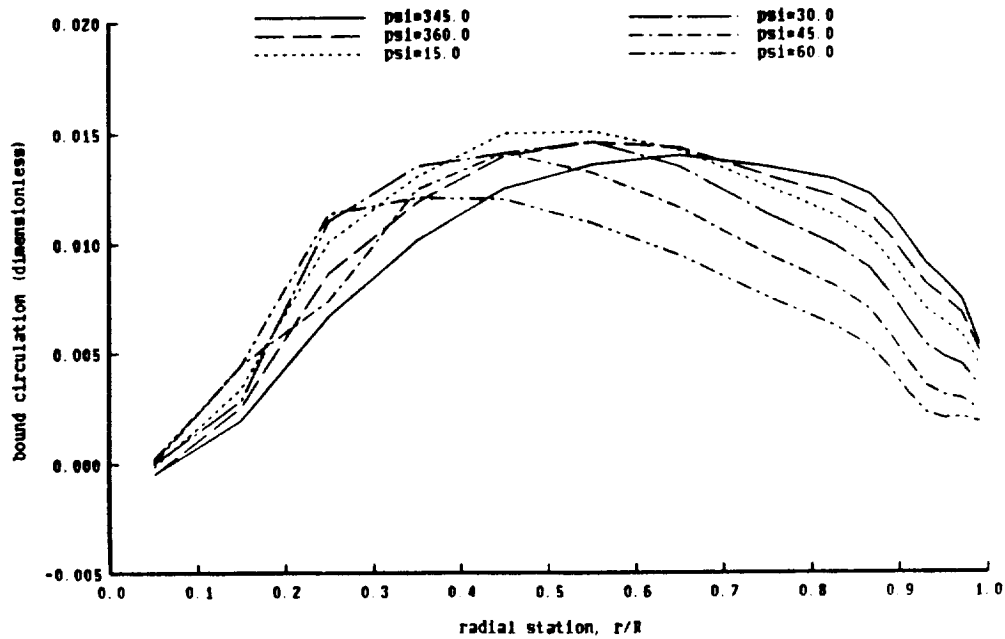
7.8.11

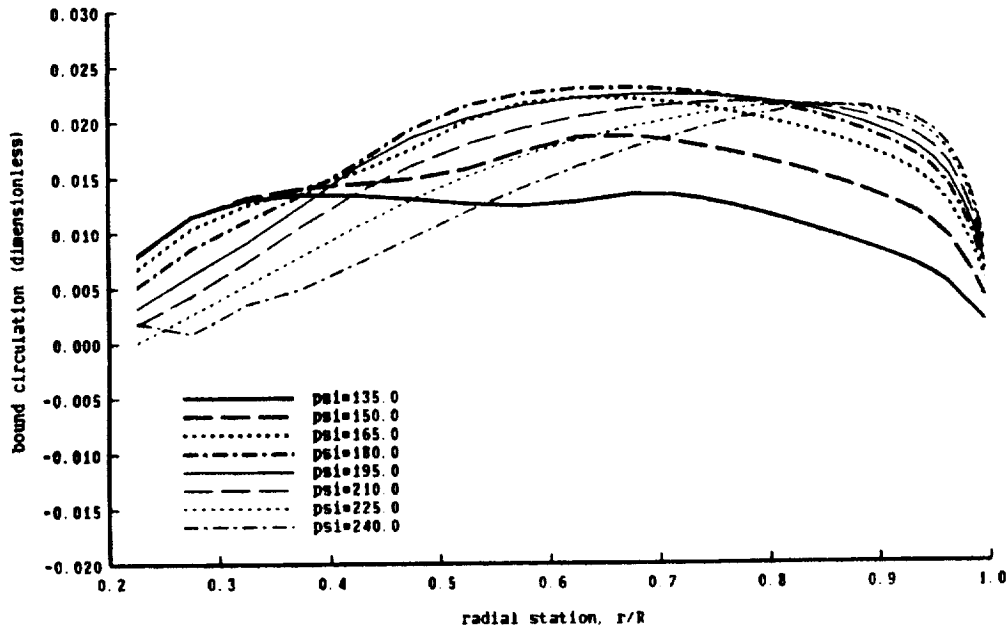ROTOR BLADE SPANWISE CIRCULATION DISTRIBUTION

4 blades, solidity = 0.082 (swept tip), nonlinear twist

V = 60 knots, CT/sigma = 0.075, X/q = 24
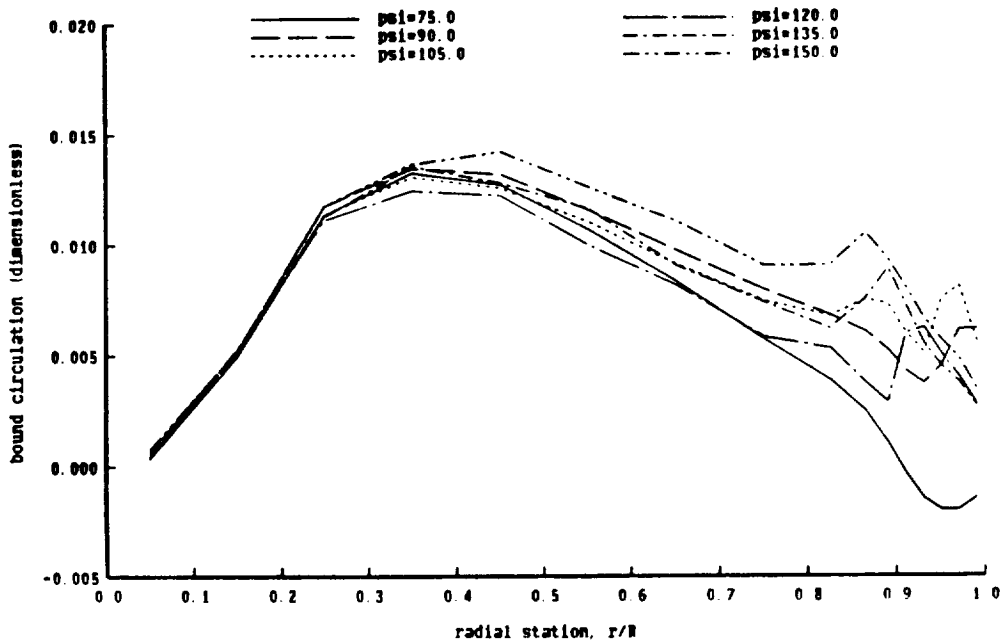
7.8.12

ROTOR BLADE SPANWISE CIRCULATION DISTRIBUTION

4 blades, solidity = 0.062, twist = -8

mu = .39, CT/sigma = .060, alpha-shaft = -5, calculated airloads

7.8.16

ROTOR BLADE SPANWISE CIRCULATION DISTRIBUTION

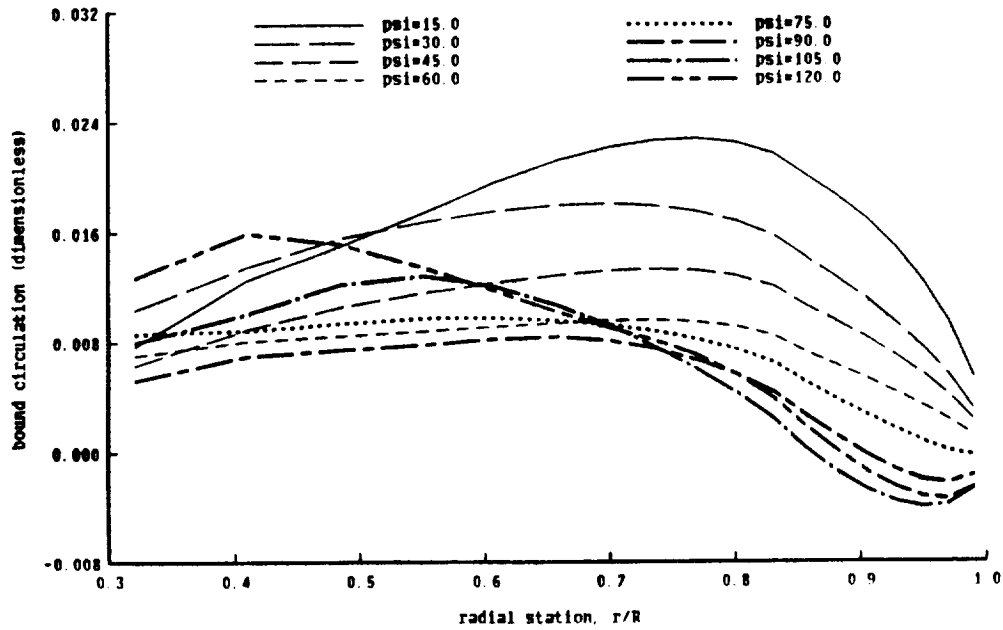4 blades, solidity = 0.092 (swept tip), twist = -9

CT/sigma = .08, mu = .37

7.8.19

ROTOR BLADE SPANWISE CIRCULATION DISTRIBUTION

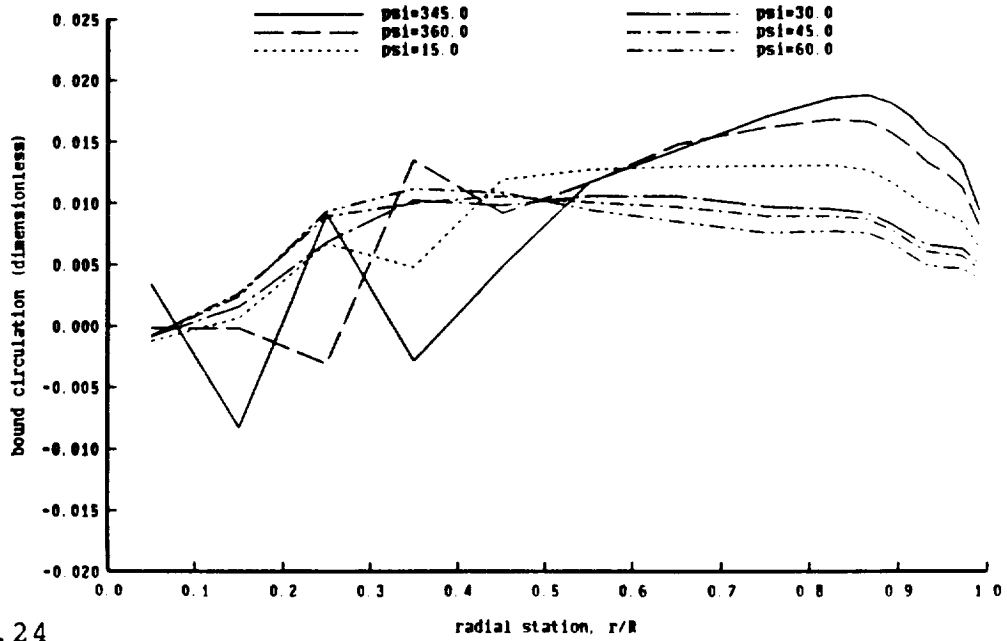4 blades, solidity = 0.107 (tapered tip)
twist = -11.7 (-17.3 for r > .86 R)

mu = .36, CT/sigma = .070, alpha-shaft = -6.7, calculated airloads

7.8.21

ROTOR BLADE SPANWISE CIRCULATION DISTRIBUTION

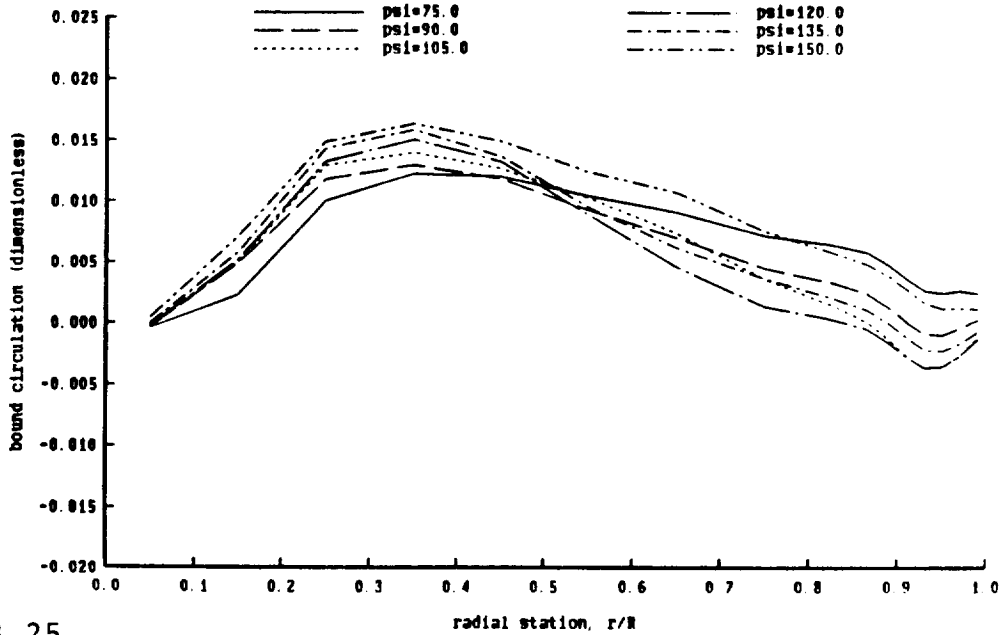4 blades, solidity = 0.082 (swept tip), nonlinear twist

V = 160 knots, CT/sigma = 0.075, X/q = 24

7.8.24

ROTOR BLADE SPANWISE CIRCULATION DISTRIBUTION

4 blades, solidity = 0.082 (swept tip), nonlinear twist

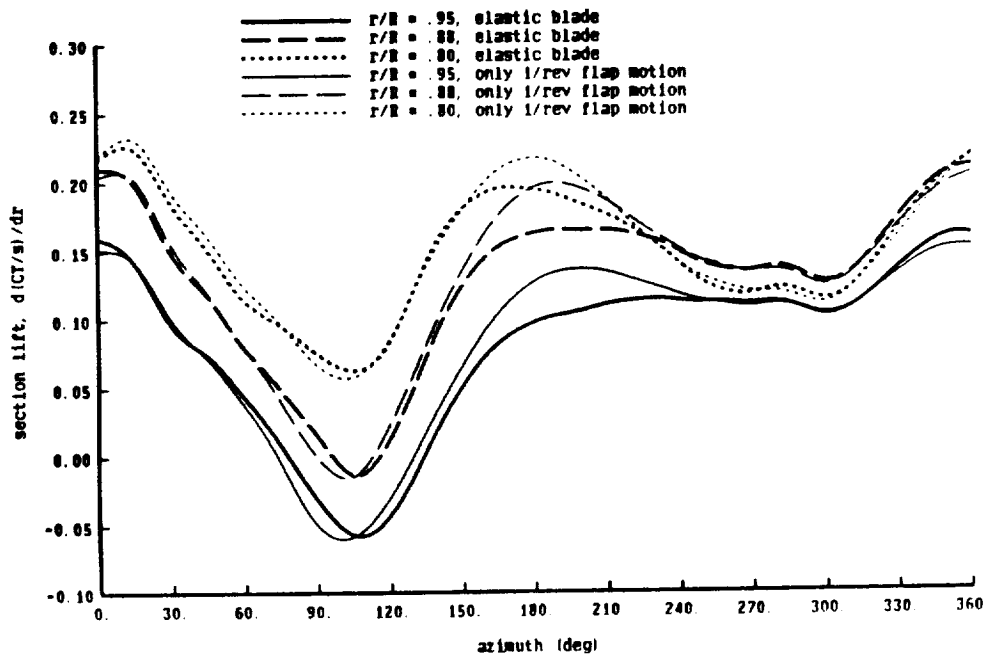V = 160 knots, CT/sigma = 0.075, X/q = 24

7.8.25

49

INFLUENCE OF BLADE ELASTIC MOTION ON AIRLOADS

4 blades, solidity = 0.107 (tapered tip)

Run 222, mu = .36, CT/sigma = .070, alpha-shaft = -6.7, dual-peak wake model
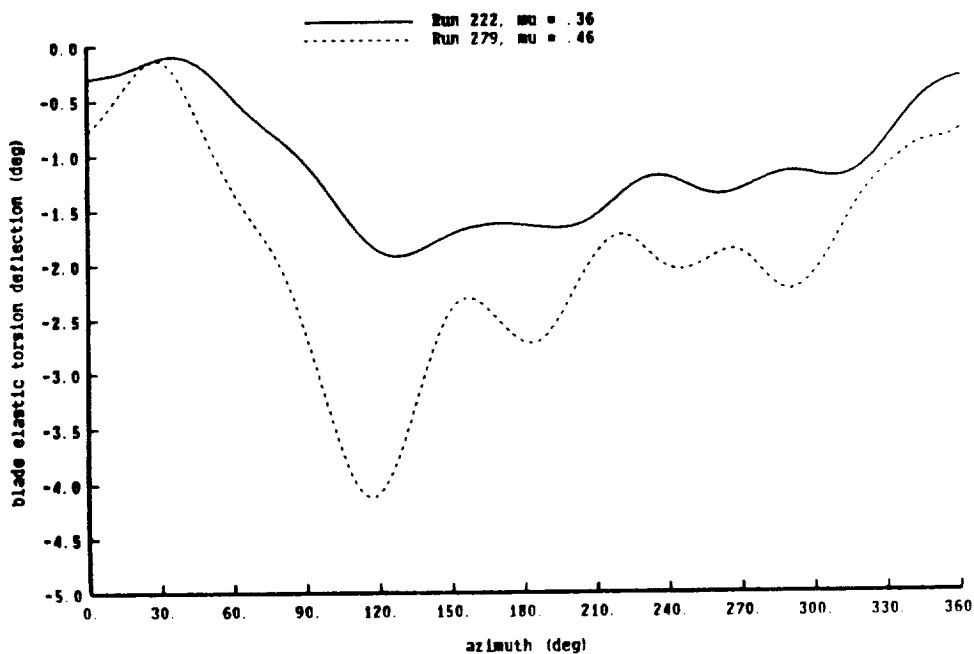

9.3.1

BLADE ELASTIC TORSION MOTION

4 blades, solidity = 0.107 (tapered tip)
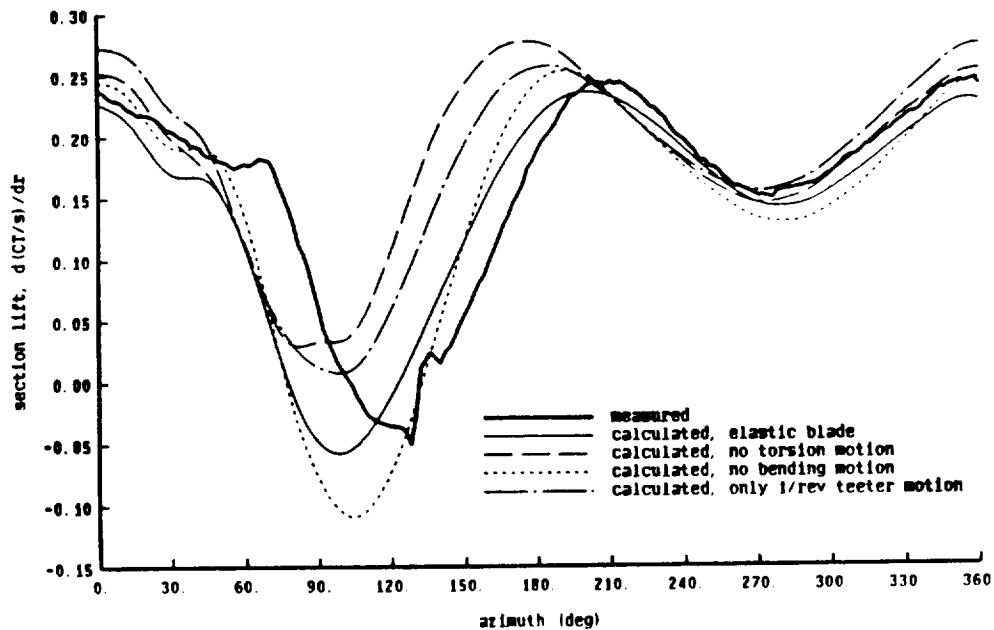
calculated blade motion, dual-peak wake model

9.3.2

INFLUENCE OF BLADE ELASTIC MOTION ON AIRLOADS

2 blades, solidity = 0.065

mu = .37, CT/sigma = .084, alpha-tpp = -6.6, r/R = .9

measured
calculated, elastic blade
calculated, no torsion motion
calculated, no bending motion
calculated, only 1/rev teeter motion

9.3.7

BLADE ELASTIC TORSION MOTION

2 blades, solidity = 0.065
= 3/rev; airfoil tables not available

calculated, NLR-1T airfoil
calculated, 10-64C airfoil
calculated, RC-SC2 airfoil
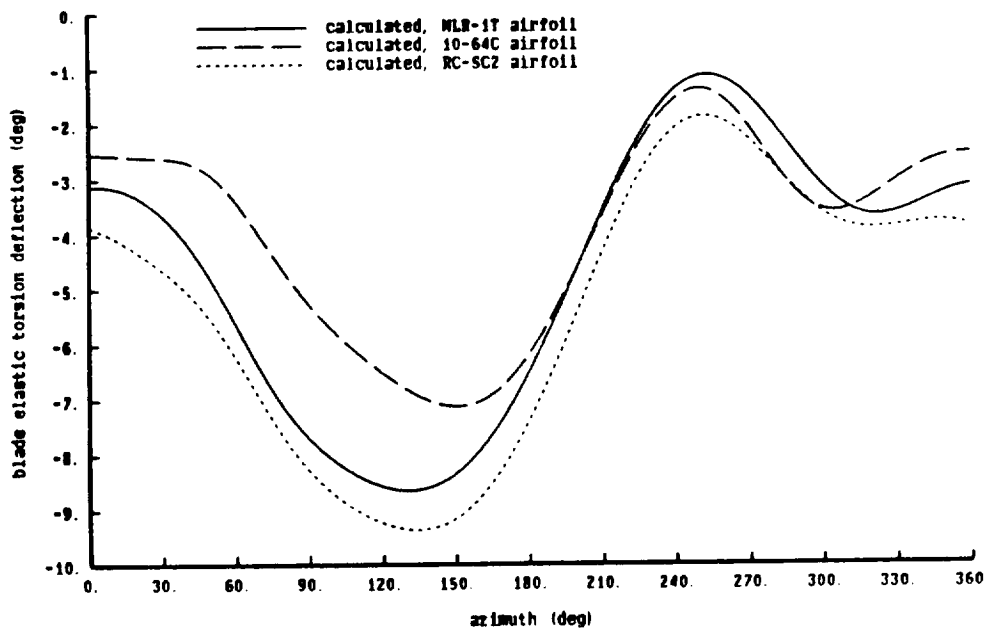
9.3.9

Report Documentation Page

1. Report No. NASA CR-177551 USAAVSCOM TM-90-A-005	2. Government Accession No.	3. Recipient's Catalog No.
4. Title and Subtitle Airloads, Wakes, and Aeroelasticity		5. Report Date April 1990
		6. Performing Organization Code
7. Author(s) Wayne Johnson		8. Performing Organization Report No. A-90165
		10. Work Unit No. 505-61-51
9. Performing Organization Name and Address Johnson Aeronautics P. O. Box 1253 Palo Alto, CA 94302		11. Contract or Grant No. NAS2-11555
		13. Type of Report and Period Covered Contractor Report
12. Sponsoring Agency Name and Address National Aeronautics and Space Administration Washington, DC 20546-0001 and U.S. Army Aviation Systems Command, St. Louis, MO 63120-1798		14. Sponsoring Agency Code

15. Supplementary Notes
Point of Contact: Chee Tung, Ames Research Center, MS 215-1, Moffett Field, CA 94035-1000 (415) 604-5241 or FTS 464-5241 Report to be presented at AGARD Special Course on Aerodynamics of Rotorcraft, von Karman Institute, Brussels, Belgium, April 2-5, 1990; Middle East Technical University, Ankara, Turkey, April 9-11, 1990; and Ames Research Center, Moffett Field, CA May 14-17, 1990.

16. Abstract
Fundamental considerations regarding the theory and modeling of rotary wing airloads, wakes, and aeroelasticity are presented. The topics covered are: (a) airloads and wakes, including lifting-line theory, wake models and nonuniform inflow, free wake geometry, and blade-vortex interaction; (b) aerodynamic and wake models for aeroelasticity, including two-dimensional unsteady aerodynamics and dynamic inflow; and (c) airloads and structural dynamics, including comprehensive airload prediction programs. Results of calculations and correlations are presented.

17. Key Words (Suggested by Author(s)) Helicopter Airloads Wakes Aeroelasticity		18. Distribution Statement Unclassified-Unlimited Subject Category – 02	
19. Security Classif. (of this report) Unclassified	20. Security Classif. (of this page) Unclassified	21. No. of Pages 54	22. Price A04